c.1

CANADA

STANDARDIZED PROCEDURES FOR THE DETERMINATION OF THE PHYSICAL PROPERTIES OF MINE ROCK UNDER SHORT-PERIOD UNIAXIAL COMPRESSION

H. R. HARDY, JR.
FUELS AND MINING PRACTICE DIVISION

DEPARTMENT OF MINES AND TECHNICAL SURVEYS, OTTAWA

MINES BRANCH

TECHNICAL BULLETIN

TB 8

PRICE 50 CENTS.

(Reissue of Fuels and Mining Practice Division Report No. FRL - 242, dated December 1957)

DECEMBER 1959

FOREWORD

The content of this bulletin was first issued in December 1957 as Report No. FRL-242 of the Fuels and Mining Practice Division describing the procedure developed prior to 1958. Owing to the wide interest with which the report was received, a reissue has become necessary. The opportunity has been taken to correct some minor errors in the original report, but no alterations have been made to take account of more recent developments.

Since FRL-242 was issued new techniques have been under study, particularly with regard to the methods of strain measurement and of applying uniform stress. Changes are also being adopted in the methods of specimen selection and data analysis. These and other modifications of the standard test procedure will be published as they become established.

A. Ignatieff, Chief,

Fuels and Mining Practice Division.

OTTAWA, December 1959.

Mines Branch Technical Bulletin TB 8

STANDARDIZED PROCEDURES FOR THE DETERMINATION OF THE PHYSICAL PROPERTIES OF MINE ROCK UNDER SHORT-PERIOD UNIAXIAL COMPRESSION

by

H.R. Hardy, Jr.*

SYNOPSIS

This bulletin describes in detail the problems encountered and the standardized methods evolved for the determination of a number of the physical properties of mine rock under short-period uniaxial compression. These properties include compression modulus, Poisson's ratio, ultimate compressive strength, fracture angle, and strain energy. In addition a number of related properties are discussed, including rock type classification, petrographic classification, apparent specific gravity, and Mohs hardness. The analysis of the data obtained for these physical properties is discussed in some detail.

*Scientific Officer, Fuels and Mining Practice Division, Mines Branch, Department of Mines and Technical Surveys, Ottawa, Canada.

Direction des mines, Bulletin technique TB 8

NORMES POUR L'ÉVALUATION DES PROPRIÉTÉS PHYSIQUES DES ROCHES MINIÈRES EN COMPRESSION UNIAXIALE BRÈVE

par

H.R. Hardy, Jr.*

RÉSUMÉ

Ce bulletin décrit en détails les problèmes qui se sont posés et les méthodes normalisées qui ont été élaborées pour l'évaluation d'un certain nombre de propriétés physiques des roches minières en compression uniaxiale de courte durée. Ces propriétés comprennent le module de compression, le coefficient de Poisson, la résistance à la rupture en compression, l'angle de fracture et l'énergie de déformation. En outre, le présent travail considère certaines propriétés du même genre telles que la classification par type de roche, la classification pétrographique, la densité apparente, et la dureté de Mohs. L'analyse des résultats obtenus pour ces propriétés physiques est étudiée en détails.

* Chargé de recherches, Division des combustibles et de la pratique minière, Direction des mines, Ministère des Mines et des Relevés techniques, Ottawa, Canada.

Mines Branch Technical Bulletin TB 8

STANDARDIZED PROCEDURES FOR THE DETERMINATION OF THE PHYSICAL PROPERTIES OF MINE ROCK UNDER SHORT-PERIOD UNIAXIAL COMPRESSION

by

H.R. Hardy, Jr.*

SYNOPSIS

This bulletin describes in detail the problems encountered and the standardized methods evolved for the determination of a number of the physical properties of mine rock under short-period uniaxial compression. These properties include compression modulus, Poisson's ratio, ultimate compressive strength, fracture angle, and strain energy. In addition a number of related properties are discussed, including rock type classification, petrographic classification, apparent specific gravity, and Mohs hardness. The analysis of the data obtained for these physical properties is discussed in some detail.

*Scientific Officer, Fuels and Mining Practice Division, Mines Branch, Department of Mines and Technical Surveys, Ottawa, Canada.

Direction des mines, Bulletin technique TB 8

NORMES POUR L'ÉVALUATION DES PROPRIÉTÉS PHYSIQUES DES ROCHES MINIÈRES EN COMPRESSION UNIAXIALE BRÈVE

par

H.R. Hardy, Jr.*

RÉSUMÉ

Ce bulletin décrit en détails les problèmes qui se sont posés et les méthodes normalisées qui ont été élaborées pour l'évaluation d'un certain nombre de propriétés physiques des roches minières en compression uniaxiale de courte durée. Ces propriétés comprennent le module de compression, le coefficient de Poisson, la résistance à la rupture en compression, l'angle de fracture et l'énergie de déformation. En outre, le présent travail considère certaines propriétés du même genre telles que la classification par type de roche, la classification pétrographique, la densité apparente, et la dureté de Mohs. L'analyse des résultats obtenus pour ces propriétés physiques est étudiée en détails.

* Chargé de recherches, Division des combustibles et de la pratique minière, Direction des mines, Ministère des Mines et des Relevés techniques, Ottawa, Canada.

CONTENTS

CONTENTS (Cont'd)

CONTENTS (Cont'd)

CONTENTS (Concluded)

FIGURES

FIGURES (Cont'd)

FIGURES (Concluded)

TABLES

INTRODUCTION

Since the beginning of this century, laboratory experiments have been conducted to investigate the behaviour of rock and mineral specimens under varying conditions of stress and time. The majority of these studies were conducted in the fields of Geology and Civil Engineering, on materials not closely related to one another and with non-standardized test procedures.

The specific investigation of the physical properties of mine rock and minerals is a branch of the science of rock mechanics. A number of excellent reports have been published on this work over the past ten years. These include, amongst others, a comprehensive study of the relationship of the physical and petrographic properties of rock and minerals to stress problems related to mining, by D. W. Phillips;[1] reports on the development of standard test procedures for determining the physical properties of mine rock, by the U.S. Bureau of Mines[2] and the U.S. Bureau of Reclamation;[3] a number of reports dealing with studies of basic physical properties of rock and minerals;[4-8] and other reports dealing more specifically with the properties of mine rock and minerals as related to underground investigations of convergence and stress phenomena.[9-10]

The Mining Research Section of the Fuels and Mining Practice Division has undertaken an extensive project dealing with strata stress problems in Canadian mines. The investigation comprises field studies conducted in the mines, supplemented by laboratory investigations into the physical properties of the rocks and minerals. Laboratory studies have been conducted along three distinct although related paths, namely, short-period uniaxial compression, long-period uniaxial compression (time-strain), and short-period triaxial compression.

The present report deals with standardization of procedures for determination of the physical properties of mine rock and minerals under short-period uniaxial compression. Although a program of studying a number of the physical properties of mine rock might at first appear to be a relatively easy task, many problems have been encountered in development of procedure and equipment, in definition of terms, and in analysis of results. In most previous reports on physical properties of similar materials, there has been little mention of test procedure, the load at which the elastic constants were calculated, and the methods employed in these calculations. Under these conditions little or no comparison of results by different workers was possible and, as a result, progress has been limited. Two reports, namely those by the U.S. Bureau of Mines(2) and the U.S. Bureau of Reclamation,(3) mentioned previously, have formulated standardized procedures to which the writer has made frequent reference. A number of results quoted in the former with reference to effect of moisture and rate of loading are quoted later in this report.

The methods discussed in this report are certainly not the only approach to the problem, nor are the techniques discussed necessarily final. It is, rather, a form of progress report written in an effort to group together the methods presently being employed at the Fuels and Mining Practice Division, so that other workers in this field may have more complete details of the research to date.

SPECIMEN SELECTION AND PREPARATION

Selection and Labeling

Specimens have been secured from diamond-drill holes and also from block samples obtained from caved sections of the underground workings. Diamond-drill cores are preferred as they provide sounder test specimens than those cut from block samples that have already failed through mining processes. Such rock samples (either core or block) have been obtained from all the mines under study in the strata stress project being conducted by the Division. The drill-core samples are selected by field officers of the Division, who furnish identification as to the location of the bore holes in the mine and as to the stratigraphic position (along the bore hole) of each point sampled.

After receipt of the drill-core samples at the Ottawa laboratories (see Figure 1), an initial selection is made of a representative number of the samples. Generally, this entails the selection of pieces of core, each from 6 to 8 inches long, at frequent intervals along the length of the core. An attempt is made to secure core lengths of this size, to allow the preparation of three adjacent specimens. These thereafter constitute a "test set" and allow results

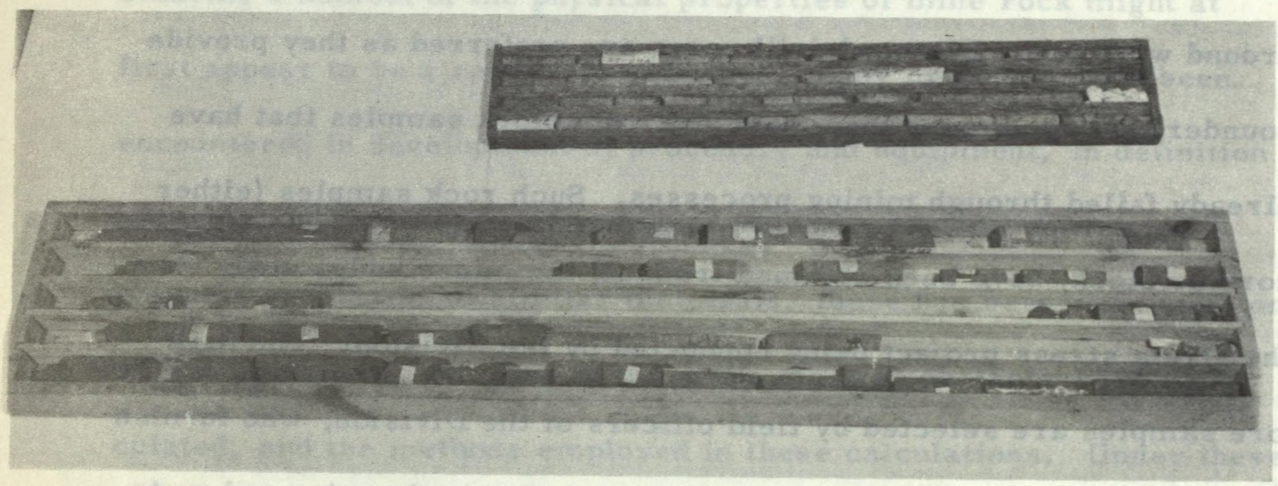

Figure 1 - Photograph showing core boxes with rock core as received from locations in the field.

at each point in the bore hole to be compared and averaged. The three components of each test set are identified by the original sample number and the sub-symbols A, B and C respectively. The specimens also bear an arrow, as illustrated in Figure 2, indicating the direction in which drilling took place (i. e., for roof holes the arrow points upwards; for floor holes it points downwards).

When the necessary rock samples have been selected the remaining core is placed in storage in the event that additional specimens may be required for future tests.

Preparation

The selected pieces of core are first cut roughly into separate right cylindrical specimens, using a rotary diamond saw with water lubrication. Specimen lengths vary with core diameter; a ratio of diameter to length of 1:1 is maintained, if possible. However, for all diameters less than 1-1/2 inches the specimen length remains fixed at 1-1/2 inches so that resistance-type strain gages may be conveniently attached to the specimen. Next, the specimens are placed in special grinding jigs, as illustrated in Figure 3, and are ground to the required length using carborundum powder and a lapidary wheel. These jigs assure that the length of the finished specimen is accurate to 1/1000 of an inch and that its ends are plane-parallel. Figure 4 shows the apparatus for specimen preparation. A number of prepared specimens are shown in Figure 5.

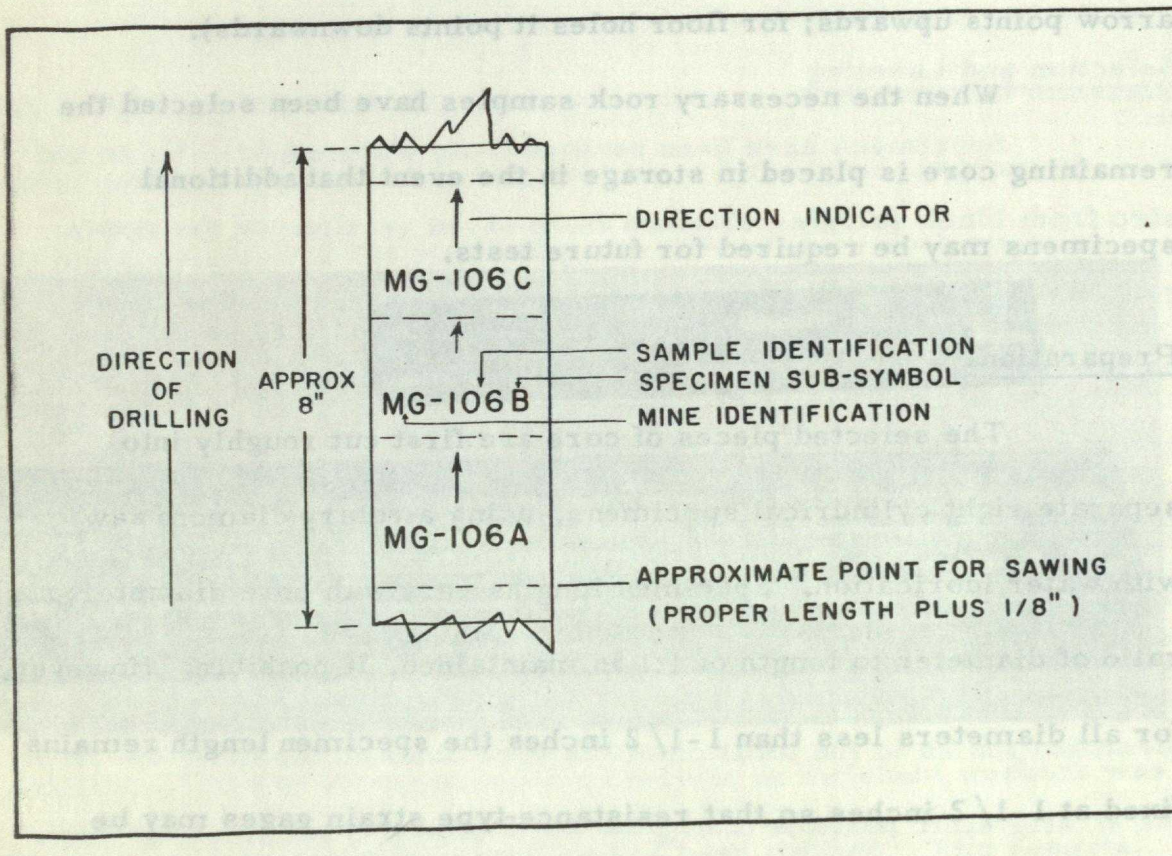

Figure 2 - Diagram illustrating the method of marking rock core samples during specimen preparation.

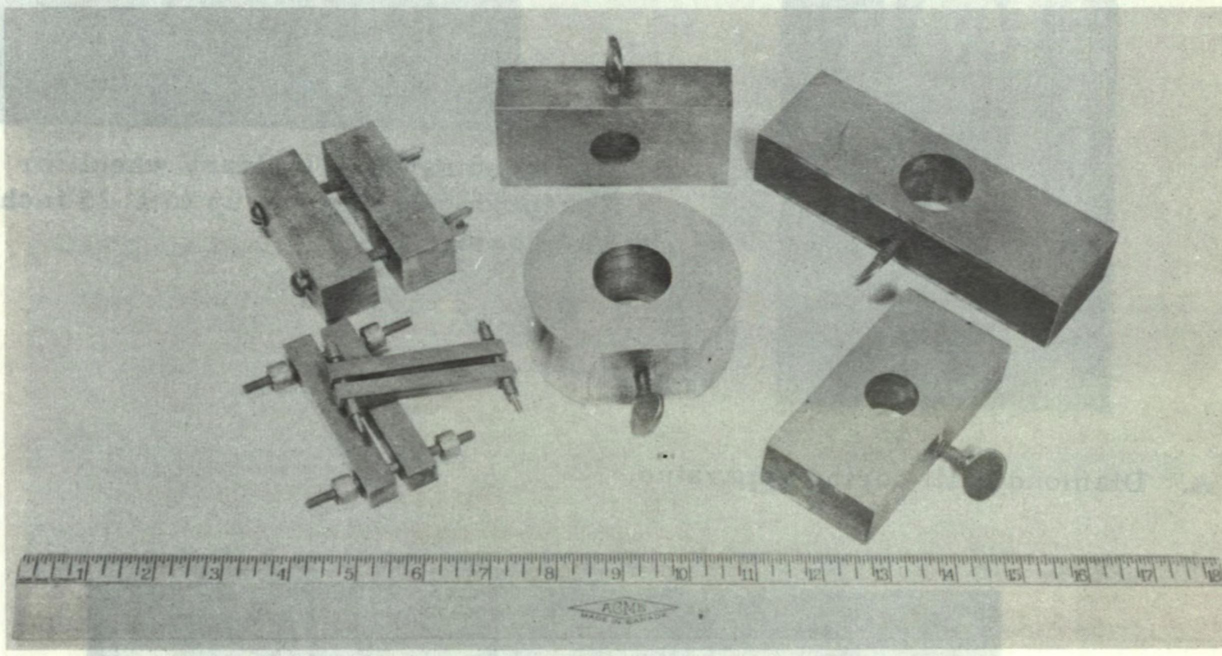

Figure 3 - Photograph showing special grinding jigs for rock specimen preparation.

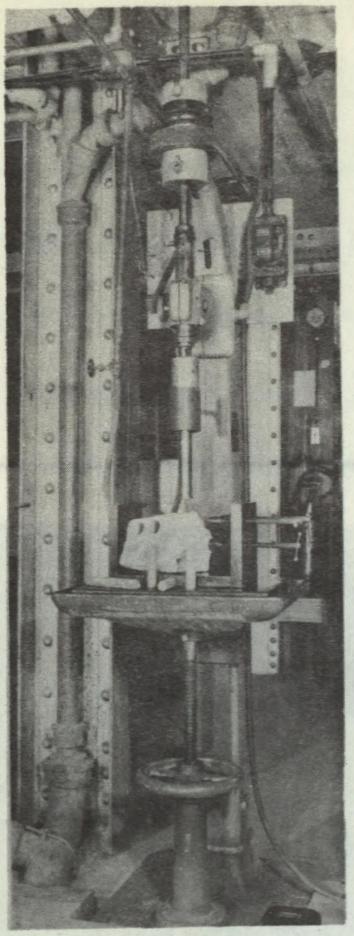

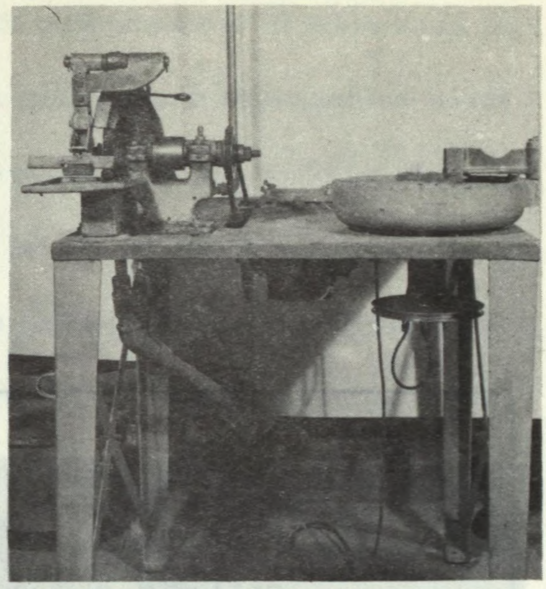

B. Diamond saw and lapidary wheel for preparing specimens up to 1.25 inches in diameter.

A. Diamond drill-coring apparatus.

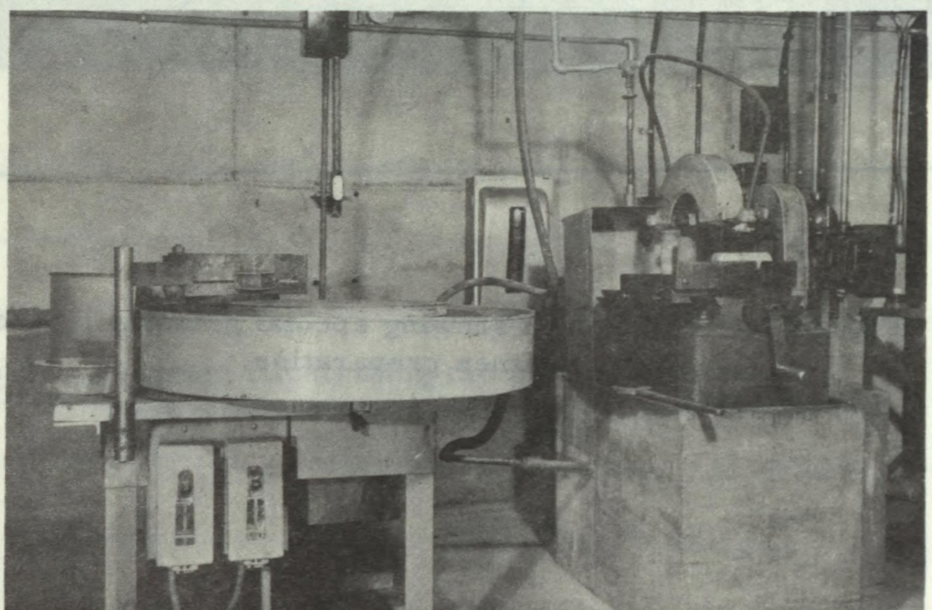

C. Lapidary wheel and diamond saw for preparing specimens larger than 1.25 inches in diameter.

Figure 4 - Photographs showing apparatus for preparation of rock specimens. (Mineral Processing Division)

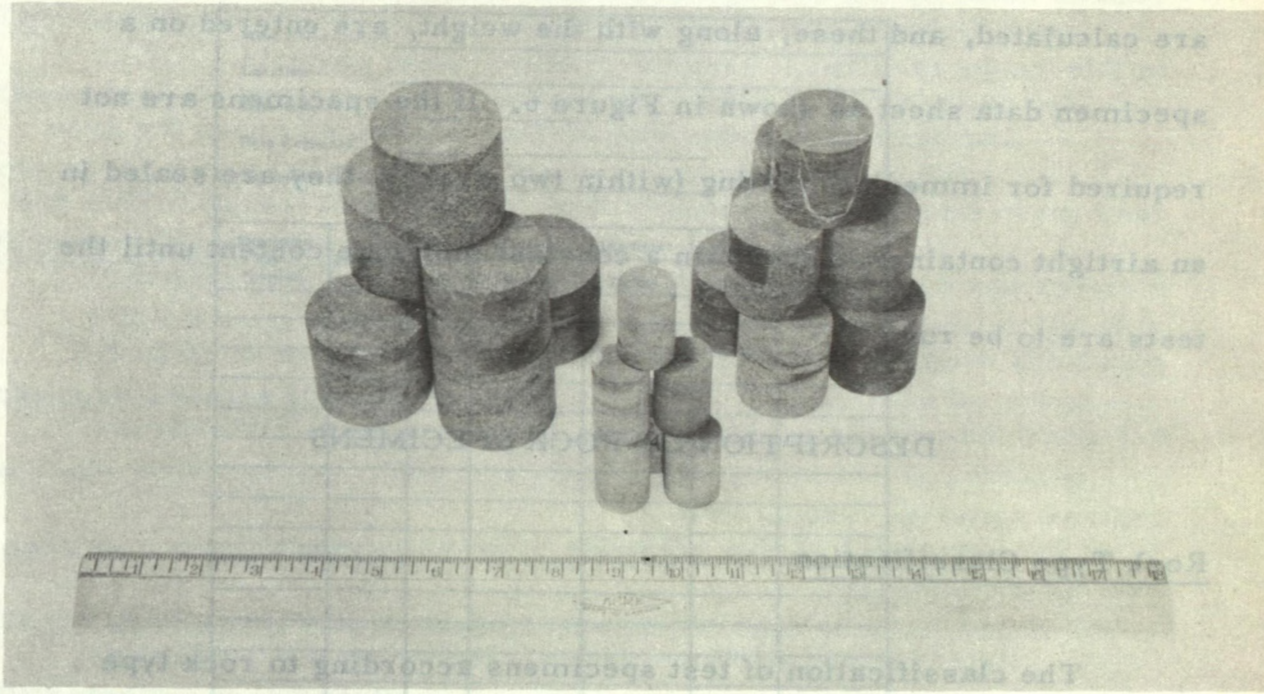

Figure 5 - Photograph showing a group of prepared rock specimens of assorted size.

After the specimens are satisfactorily ground they are allowed to dry for two weeks at room temperature to remove excess moisture. Each specimen is then measured, to an accuracy of 1/1000 of an inch, at five points for length and six points for diameter, and then weighed to the nearest milligram. The average values of length and diameter are calculated, and these, along with the weight, are entered on a specimen data sheet as shown in Figure 6. If the specimens are not required for immediate testing (within two weeks), they are sealed in an airtight container to maintain a constant moisture content until the tests are to be run.

DESCRIPTION OF ROCK SPECIMENS

Rock Type Classification

The classification of test specimens according to rock type was carried out using the simple scratch test together with visual examination of the prepared specimen. It is felt by the writer that this crude method of classification is too open to human error, and this has been exemplified by differences in the classification of a single section of rock strata by the field geologists of the Geological Survey of Canada and the staff of the Mining Research Section.[11] However, this method of classification will be employed pending the development of a more satisfactory technique.

The specimens were first grouped into four main classifications: shale, sandy shale, sandstone, and conglomerate. The

SPECIMEN DATA SHEET

Mine ------------ ____________________

Location -------- ____________________

Bore Hole ------- __________

Date Prepared ---- _______________

Technician ------- _______________

Specimen Lab. Number	Footage	Rock Type	Length Inches	Diameter Inches	Weight Lb	Density Lb / $inch^3$

Figure 6 - Specimen data sheet for recording dimensions and weights of prepared rock specimens.

distinction between shale, sandstone and conglomerate can be accomplished fairly readily. However, the intermediate materials lying between shale and sandstone are difficult to classify; from studies made by the Geological Survey, it appears that classification in this range is difficult even using thin-section analysis.

The sandstone group was further subdivided under the arbitrary grain size classifications of fine, medium and coarse. This subdivision was done macroscopically, by comparison with selected standards whereby those having mean grain diameters of up to 0.2, 0.5 and 0.88 mm were classified as fine-, medium- and coarse-grained material respectively.

Petrographic Studies

Petrographic studies were carried out by the Geological Survey of Canada on selected rock specimens from the mines under study. These tests were performed in an effort to improve the classification technique and in order to obtain greater detail on the type of rock under examination.

A representative set of specimens from each mine area under study was selected from the fracture fragments of the test specimens following the failure tests. An attempt was made to select one specimen from each of the major strata groups. These were forwarded to the Geological Survey of Canada, where the following properties were determined:

Rock type
Major and minor constituents
Grain size
Cementing material
Percentage of grains to cementing material
Type and degree of structure present.

Thin sections were prepared and photomicrographs taken of the characteristic types. These photographs, along with the other petrographic data, are included in the final report for each mine.

Apparent Specific Gravity

The apparent specific gravity was obtained, in the majority of cases, by dividing the weight of the specimen in grams by its volume in cubic centimetres. This is a simple procedure and is probably open to a small degree of error, since the value of volume used in these calculations was obtained from the average value of length and diameter for each specimen.

A more refined technique was employed for the measurement of specific gravity of irregularly shaped specimens.[2] The specimen was first weighed in air, then weighed while suspended in water, and finally the wet specimen was weighed in air. The apparent specific gravity* (ASG) was then determined, as follows:

$$ASG = \frac{M_1}{M_3 - M_2},$$

where M_1 = weight of dry specimen in air, in grams;

* This is termed apparent specific gravity since it assumes that no voids exist within the specimen which would introduce an error in the calculation of specimen volume.

M_2 = weight of specimen immersed in water, in grams ; and

M_3 = weight of wet specimen after water immersion, in grams.

Mohs Hardness

The relative hardness of all rock specimens tested was classified according to the Mohs hardness scale. This test was established by Mohs (1824), who proposed ten minerals in increasing order of scratch hardness. These are: 1. talc, 2. gypsum, 3. calcite, 4. fluorite, 5. apatite, 6. orthoclase, 7. quartz, 8. topaz, 9. corundum, and 10. diamond. Each mineral will scratch the one on the scale below it, but will not scratch the one above it.

A set of the above minerals was used to obtain the Mohs hardness of each test specimen. The hardness check was usually made on one of the plane ends of the fractured test specimens after all tests were completed.

APPARATUS

Introduction

The apparatus for obtaining values of compression modulus and Poisson's ratio consists of a Martens mirror extensometer, for measuring longitudinal strain, and SR-4 resistance-type strain gages with a Baldwin strain indicator bridge, for measuring transverse strain. A standard compressional testing machine was used to apply the necessary loads to the test specimen.

Martens Mirror Extensometer

1. General Theory

The longitudinal compression of the rock specimens was measured by a physical-optical apparatus known as the Martens mirror extensometer.[12] Photographs of this apparatus are shown in Figure 7, and Figure 8 illustrates the operation of the mirror system. The rock specimen (Sp) is placed between the two steel cylinders (A1 and A2), this being necessary since the gage length (K) of the comparison strip was greater than the specimen length (H). The comparison strips (C) (two are used to help correct for off-centre loading) are placed along the specimen, diametrically opposite to each other. Knife edges at their upper ends grip the steel capping pieces as shown. The movable knife edge (N), with its attached mirror, is set between the lower cap piece and the groove in the comparison strip. The telescope is first centred on the mirrors, then the mirrors themselves are adjusted to throw an image of the scale back through the telescope. As the specimen is compressed the mirror (being held by the comparison strip at one end) tilts, and the observer sees the reflected scale moving past his field of vision. This observed change in scale reading (or scale deflection) is proportional to the compression of the rock specimen, the constant of proportionality depending only on the geometry of the optical system.

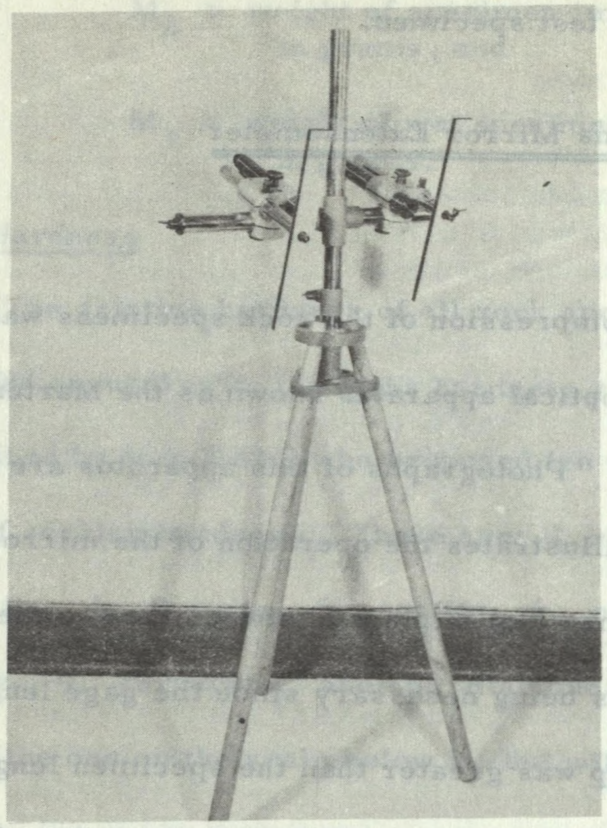

A. Martens mirror extensometer, telescope, and scales.

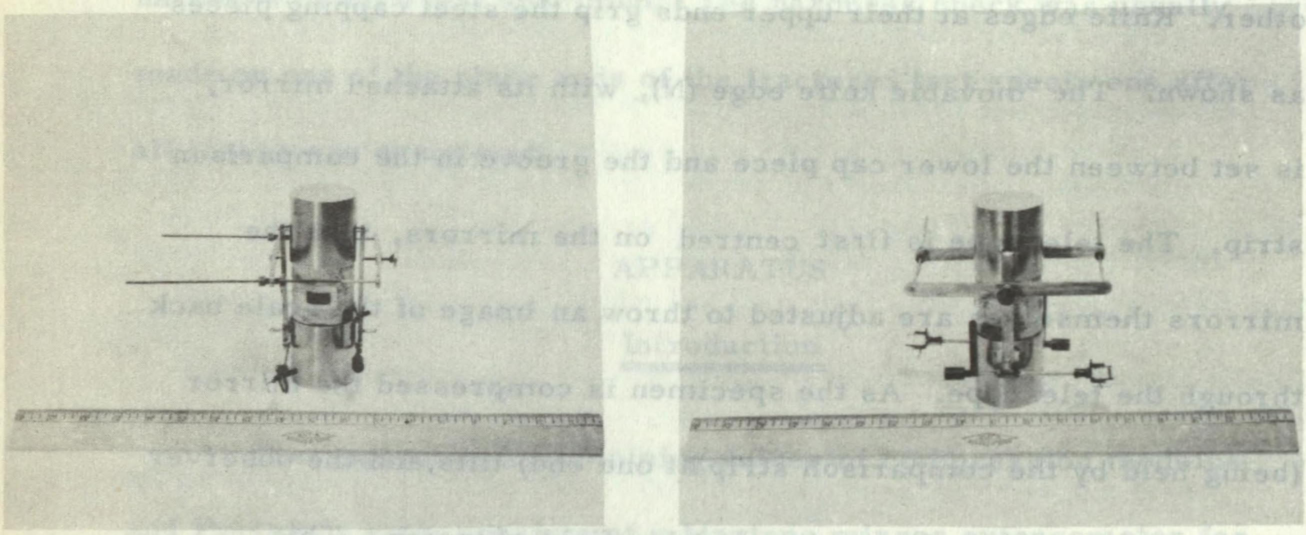

(Front view) (Side view)

B. Martens mirror extensometer attached to steel capping cylinders above and below rock specimen, showing side and front views of mirrors and knife edges.

Figure 7 - Photographs showing Martens mirror extensometer.

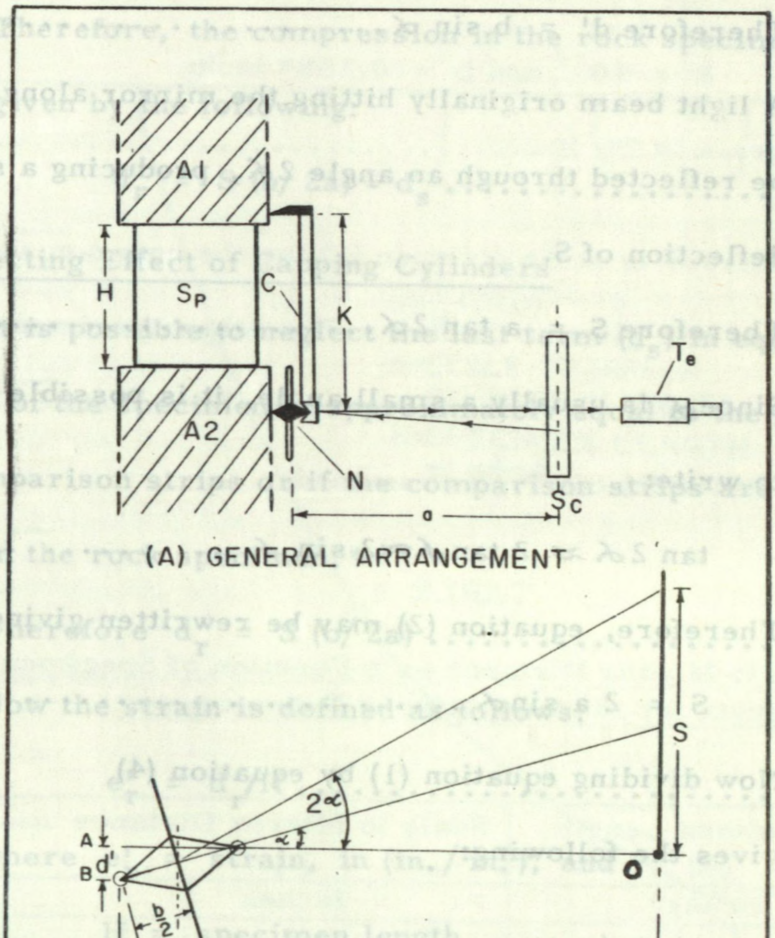

(A) GENERAL ARRANGEMENT

(B) DIAGRAM FOR THE DERIVATION OF MARTENS MIRROR FORMULA.

Figure 8 - Diagram illustrating the operation of the Martens mirror extensometer.

The constant may be calculated from Figure 8. Let the specimen and capping pieces be compressed an amount AB. The knife edges will then have moved a distance d', and the normal to the mirror will have turned through an angle α.

Therefore $d' = b \sin \alpha$ .... (1)

A light beam originally hitting the mirror along OA will be reflected through an angle 2α, producing a scale deflection of S.

Therefore $S = a \tan 2\alpha$ .... (2)

Since α is usually a small angle, it is possible to write:

$\tan 2\alpha \approx 2 \tan \alpha \approx 2 \sin \alpha$ .... (3)

Therefore, equation (2) may be rewritten giving

$S = 2a \sin \alpha$ .... (4)

Now dividing equation (1) by equation (4) gives the following:

$d' = S(b/2a)$ .... (5)

where d' = compression in specimen and capping pieces,

S = observed scale deflection,

b = width of knife edges, and

a = scale to mirror distance.

Note: All dimensions are in inches unless otherwise stated.

In general, however, d' is the sum of two parts.

$$d' = d_r + d_s \qquad (6)$$

where d_r = compression in rock specimen,

d_s = compression in capping material.

Therefore, the compression in the rock specimen (d_r) is given by the following:

$$d_r = S\,(b/2a) - d_s \qquad (7)$$

2. <u>Neglecting Effect of Capping Cylinders</u>

It is possible to neglect the last term (d_s) in equation (7) if the length of the specimen is approximately equal to the gage length of the comparison strips or if the comparison strips are placed directly on the rock specimen.*

Therefore $d_r = S\,(b/2a) \qquad (8)$

Now the strain is defined as follows:

$$e'_r = d_r/H \qquad (9)$$

where e'_r = strain, in (in./in.), and

H = specimen length.

Substituting (8) into (9) gives:

$$e'_r = Sb/2aH \qquad (10)$$

or

$$e'_r = Sk \qquad (11)$$

where $k = b/2aH \qquad (12)$

---

* No comparison strips of gage length less than 2.0 inches were available when these tests were conducted.

For convenience in calculation, the factor k should be some simple number (say 10^{-3}). Assuming this value, it is possible to calculate the corresponding scale to mirror distance (a), i.e.

from (12) $a = b/2kH$

Now $k = 10^{-3}$, and $b = 0.158$* inch;

therefore, $a = 79/H$ .... (13)

Values of the mirror to scale distance (a) for the common specimen lengths employed are given in Table 1. For other specimen lengths the factor may be determined from Figure 9. Note that in all cases a magnification factor (k) of 10^{-3} is assumed.

TABLE 1

Scale to Mirror Distance as a Function of Specimen Length for Martens Mirror Extensometer

Specimen Length (H) Inches	Scale to Mirror Distance (a) Inches
1.00	79.0
1.25	63.2
1.50	52.6
1.75	45.2
2.00	39.5
2.15	36.7

In practice, however, the strain is most conveniently expressed in units of (in/in) x 10^{-6}.

* The value for (b) which is the width of the extensometer knife edges is given by the manufacturer.

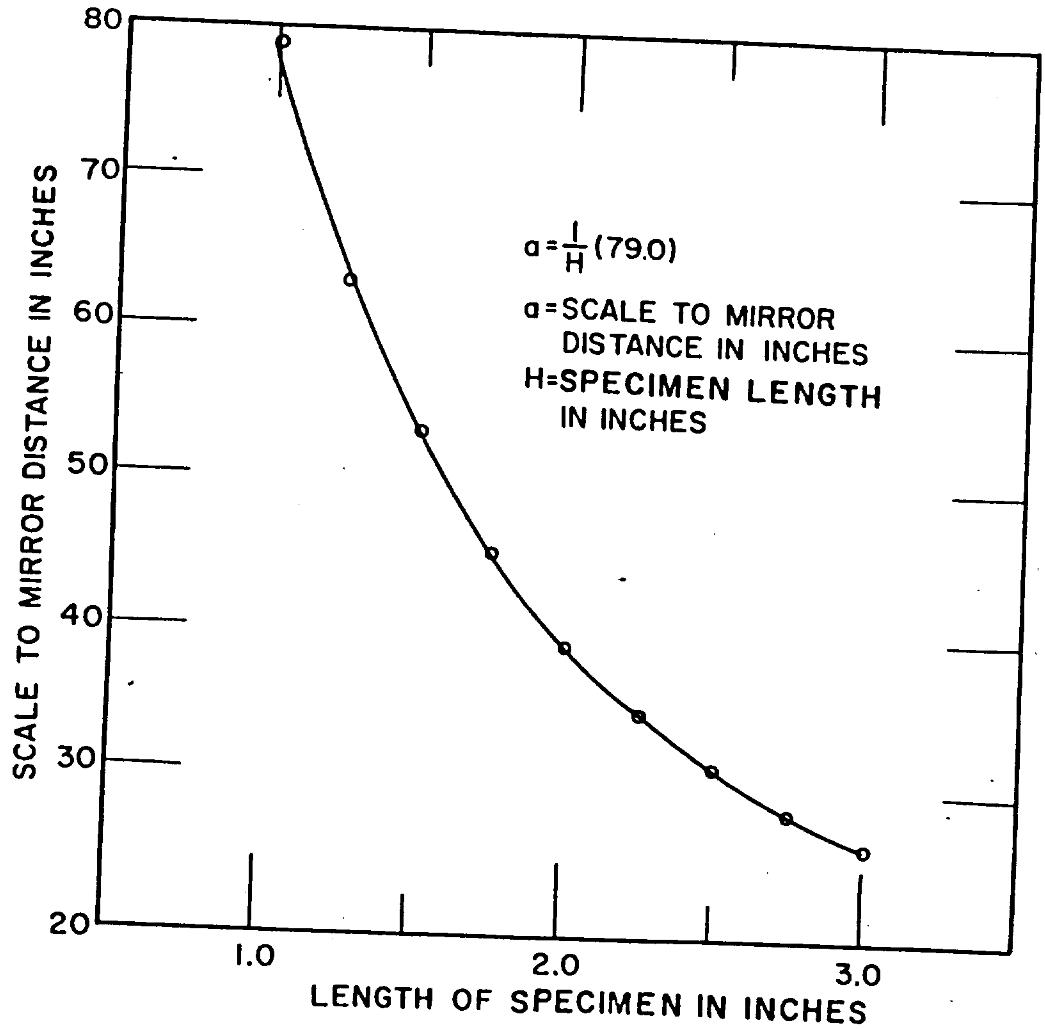

Figure 9 - Scale to mirror distance versus specimen length for Martens mirror extensometer.

Therefore $e_r = 10^6 e_r'$.

From (11), $e_r = 10^6 Sk = S\,(10^6 \times 10^{-3})$

or $e_r = 1000\,S$ .... (14)

where e_r = strain in (in/ in) x 10^{-6}, and

S = observed scale deflection.

3. Correction for Capping Cylinders

In the previous section the effect of compression in the steel capping cylinders was neglected (since $d_s \ll d_r$). However, this may not always be possible, and it is therefore necessary to determine the relationship between d_s and d_r as a function of (a) the compression modulus of steel and the test specimen and (b) the geometry of the test system. Assuming that both the rock specimen and the steel capping cylinders have a linear stress-strain curve, then:

$E_r = P/e_r$ .... (15)

and $E_s = P/e_s$ .... (16)

where E_r = Young's modulus of rock specimen (compression modulus),

e_r = strain in rock specimen due to stress P,

E_s = Young's modulus of steel,

e_s = strain in capping cylinders due to stress P, and

P = applied stress.

Rewriting equations (15) and (16) in terms of deformation gives:

$$d_r = PH/E_r \text{ .... } (17)$$

and $$d_s = P(K-H)/E_s \text{ .... } (18)$$

where K = gage length of comparison strip, and

H = length of test specimen.

Let R be defined as the ratio of the longitudinal deformation in the steel capping pieces to that in the rock specimen at the same load.

Therefore $$R = d_s/d_r \text{ .... } (19)$$

Substituting (17) and (18) into (19) gives:

$$R = (E_r/E_s)\,(K-H)/H \text{ .... } (20)$$

From (7), $$d_r/H = (S/H)\,(b/2a) - d_s/H \text{ .... } (21)$$

Substituting (19) into (21) gives:

$$d_r/H = (S/H)\,(b/2a) - R\,d_r/H$$

or $$d_r\,(1+R)/H = (S/H)\,(b/2a).$$

Now, since $e'_r = d_r/H$ from (9),

therefore $$e'_r = (S/H)\,(b/2a).\,1/(1+R) \text{ .... } (22)$$

or $$e'_r = (S/H)\,(b/2a)\,R' \text{ .... } (23)$$

where $$R' = 1/(1+R) \text{ .... } (24)$$

Now, following the same procedure as used to transform equation (10) into (14), equation (23) may be written as follows:

$$e_r = 1000\, S\, R' \quad \ldots\ldots\ldots\ldots\ldots\ldots\ldots\ldots \quad (25)$$

where e_r = strain in (in/in) x 10^{-6},

$R^1 = 1/(1 + R)$, and

$R = (E_r/E_s)\,(K-H)/H$

From equations (20) and (24) it is observed that the value of R' varies as the factor (K-H)/H, which itself varies with H, K being a parameter. To show the variation of the factor R' with H, a graph of R' vs H was prepared as follows. First, the value of R was calculated by equation (20) for gauge lengths of K = 2.0 inches and 4.0 inches, with values of H varying from 0 to 4.0 inches. Then the values of R' were calculated from equation (24), using the particular value of R previously found. These calculated values are shown graphically in Figure 10 and listed in Table 2.

It was decided to apply the correction factor R' only if R' $\leq$ 0.90. An error of at least 10% is therefore possible in observed strain values. If in the future the experimental validity of correction factor relationship is verified, then all results for specimens with K $>$ H will be corrected.

4. Sample Calculations

Consider a group of rock specimens 1.0 inch in length which are to be tested. The following example illustrates the calculation of the appropriate constants:

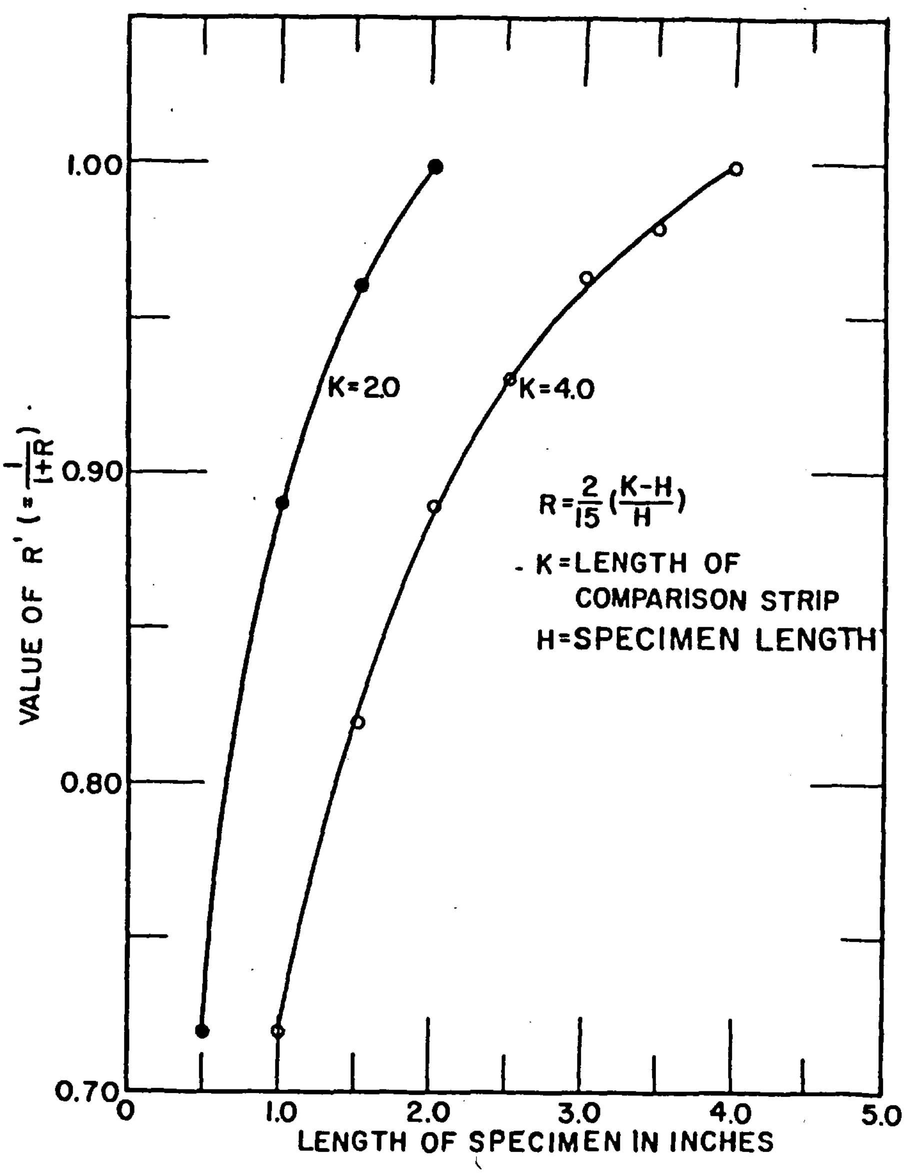

Figure 10 - Correction factor (R') versus specimen length for Martens mirror extensometer.

TABLE 2

Variation of R and R' with Specimen Length for Martens Mirror Extensometer

K= 2			K = 4		
H	R	R'	H	R	R'
0.0	-	0	0.0	-	0
0.5	0.39	0.72	0.5	0.93	0.52
1.0	0.13	0.89	1.0	0.39	0.72
1.5	0.04	0.96	1.5	0.22	0.82
2.0	0.00	1.00	2.0	0.13	0.89
			2.5	0.08	0.93
			3.0	0.04	0.96
			3.5	0.02	0.98
			4.0	0.00	1.00

where $R' = 1/(1 + R)$

$R = (E_r / E_s)\ (K-H)/H$

E_r - taken as 4.0×10^6 lb/in^2

E_s - taken as 30.0×10^6 lb/in^2

H = specimen length, in inches

K = comparison strip length, in inches.

(i) From equation (13) it is found* that the scale to mirror distance should be 79.0 inches for a specimen 1.0 inch in length.

(ii) The shortest available comparison strip is 2.0 inches in length (K = 2.0) and the specimen length is 1.0 inch (H = 1.0). Now using equation (20), R is calculated* and found to be 0.13.

(iii) Next, R' is calculated* from equation (24) and found to be 0.89.

*The values of a , R and R' could have been found directly from the tables or figures. However, for the purpose of illustration the values were worked out from the basic formulae.

Now, as $R' < 0.90$ it is necessary to apply the correction factor, and the strain is given by equation (25), namely $e_r = S\,(1000)\,(0.89)$, where S is the scale deflection observed with a mirror to scale distance of 79.0 inches.

5. Effects of Low Stresses

It is observed that low values of compression modulus are obtained at stresses of 500 to 3000 lb/ in^2. It is suspected that these low values result from the large apparent strains produced upon initial loading. These are probably due to play between the capping plates and the test specimen. For this reason, values of compression modulus obtained using the Martens' extensometer below 3000 lb/ in^2 are not considered accurate enough for comparison or for use in calculations.

Strain Gage Apparatus

1. Description of Strain Gages

Transverse strain in the cylindrical test specimens was measured by A-5 and A-7 type SR-4 resistance strain gages cemented around the circumference of the specimen (in Appendix B it is shown that the strain on the circumference of a cylindrical test specimen is equal to the transverse (diametric) strain). A detailed explanation of strain gage design and measurement technique will not be given here, as such information is available from other sources.[13, 14] However, for completeness a brief description is included.

The basic principle of the SR-4 resistance-type strain gage is extremely simple. Essentially, all gages consist of a length of very fine wire arranged in a particular pattern and bonded to a paper base. The gages are made in many sizes and shapes, depending on the particular application. In use the gage is cemented firmly to the test specimen and thus is strained uniformly with it. The resistance of the gage varies with the specimen strain, showing decreased resistance with compression of the specimen. This resistance change is measured very accurately with a special Wheatstone bridge calibrated directly in strain, in microinches/ inch.

There are three important quantities associated with each strain gage, namely:

(i) Resistance (R) = the d. c. resistance of the gage. This is usually of the order of 120 ohms.

(ii) Length (L) = the physical length of the gage winding.

(iii) Gage Factor (F) = $(\Delta R/R)/(\Delta L/L)$. For most gages this is approximately 2. 0.

2. Description of Strain Indicator Bridge

The variation of strain (i. e. variation of gage resistance) was measured by a portable Baldwin (model-L) strain indicator as shown in Figure 11. This is a battery-operated double bridge unit which indicates the magnitude and direction of an observed strain. In the test setup, two arms of the bridge were SR-4 strain gages. One, the active gage R_a, provided the strain sensing element ; the other,

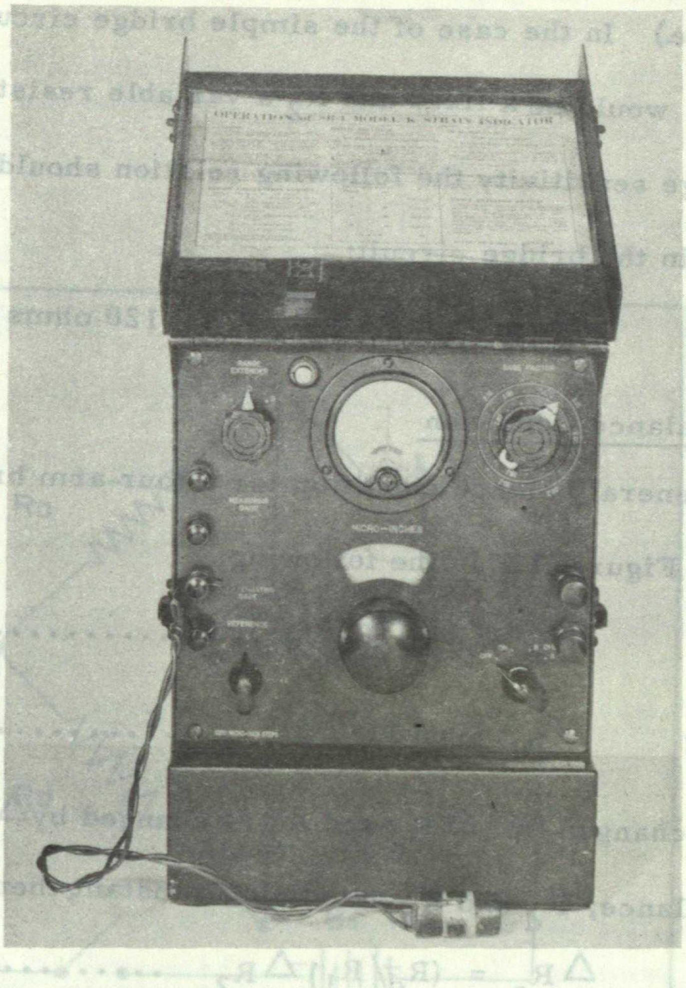

Figure 11 - Baldwin (Model-L) portable strain indicator used for measurement of lateral strain in rock specimens. (An attached dummy specimen is also shown at the base of the instrument.)

R_d, provided the necessary temperature compensation. (The variation of resistance in the dummy gage, due to temperature changes in the surroundings, tends to cancel out variations due to temperature in the active gage.) In the case of the simple bridge circuit shown in Figure 12, R_1 would be a fixed and R_2 a variable resistor. For the greatest bridge sensitivity the following relation should exist between the resistors in the bridge circuit:

$$R_1 \approx R_2 \approx R_d \approx R_a \approx R = 120 \text{ ohms} \;\ldots\ldots\; (26)$$

3. Bridge Balance Condition

The general balance condition for a four-arm bridge, as illustrated in Figure 12, is the following:

$$R_a R_1 = R_2 R_d \;\ldots\ldots\ldots\ldots\ldots\ldots\; (27)$$

giving

$$R_a = (R_d / R_1)\, R_2 \;\ldots\ldots\ldots\ldots\; (28)$$

Now, if R_a is changed by ΔR_a and R_2 is changed by ΔR_2 in order to restore balance, R_d and R_1 remaining constant, then:

$$\Delta R_a = (R_d / R_1)\, \Delta R_2 \;\ldots\ldots\ldots\ldots\; (29)$$

Since

$$F = (\Delta R / R) / (\Delta L / L) = 2.0,^* \;\ldots\ldots\; (30)$$

with $R = R_a$, this gives:

$$\Delta R_a = 2.0\, (\Delta L / L)\, R_a \;\ldots\ldots\ldots\ldots\; (31)$$

Setting equation (31) equal to (29), and noting that a change ΔR_a in the gage must be balanced by a change ΔR_2 in the bridge balancing

---

* The gage factor varies between different types of gages and between different batches of the same type. However, an average value for the A-5 and A-7 types employed in these tests is 2.0.

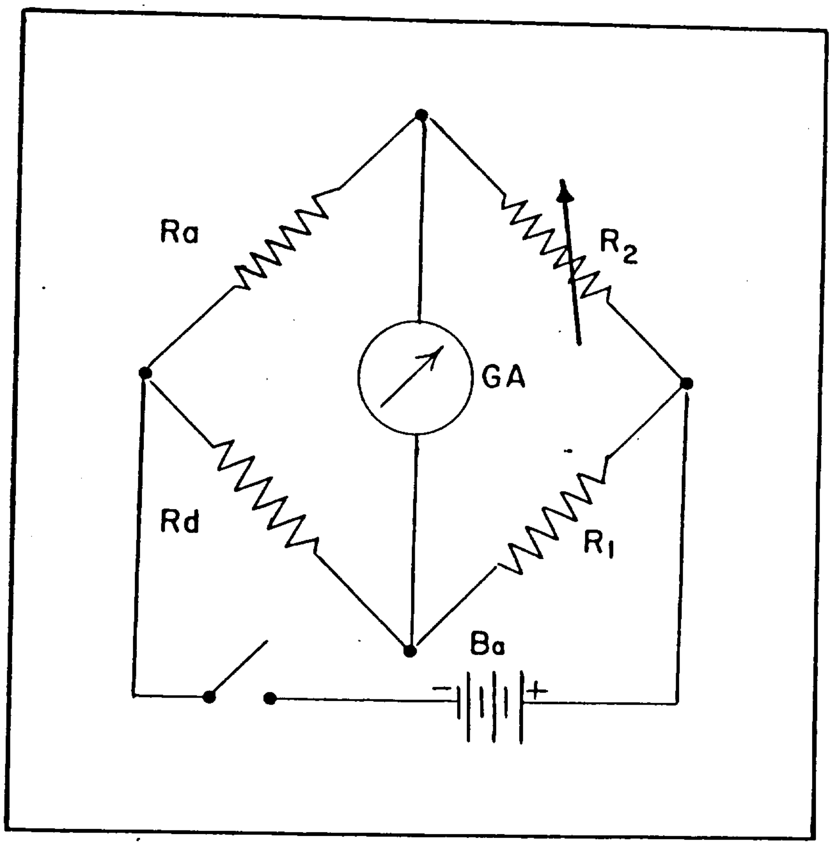

LEGEND - Ra = Active Gage
Rd = Dummy Gage
R_1 = Fixed Resistor
R_2 = Balancing Resistor
Ga = Galvanometer
Ba = Battery

Figure 12 - Simple strain gage indicator circuit (Wheatstone bridge).

resistor R_2, then

$$2.0\ (\Delta L/L)\, R_a = (R_d/R_1)\Delta R_2,$$

giving $\Delta L/L = 1/2\, (R_d/R_a R_1)\Delta R_2$ .... (32)

Since $e = \Delta L/L$

where e = strain in inches/inch,

therefore, $e = M\Delta R_2$, ... (33)

where $M = 1/2\, (R_d/R_a R_1) \approx 1/240$ ...... (34)

Equation (33) makes it possible to calculate the strain from the observed variations in gage resistance and the constant M.

It was not necessary to calculate the strain in this manner for the present series of tests, since a commercial bridge was available which was calibrated directly for strain in microinches/inch.

4. Automatic Averaging of Two Strain Gage Measurements

Due to the heterogeneity of materials such as rock, plus the possibility of eccentric loading of the test specimen, it was considered necessary to use two strain gages, mounted diametrically opposed to each other, for the measurement of transverse strain. During the initial tests, the variation of strain with load was observed separately for each gage and the average was taken. However, to reduce the time for testing and calculation, the two gages were connected in series in later tests, together with a double dummy gage, to give automatic averaging. This automatic averaging is possible because of the form of equation (28) and is explained in detail in Appendix A.

5. Procedure for Attaching Strain Gages to Rock Specimens

Since strain gages are sensitive to moisture, temperature, and mechanical disturbances, special precautions must be taken in applying gages to rock specimens so that consistent results will always be obtained. The following procedure was developed:

(i) The specimens were cleaned of all dirt and grease, then dried at room temperature in the laboratory for a period of not less than two weeks.

(ii) The surface of the rock specimen (where the gage was to be attached) was roughened with coarse emery paper and/or steel wool. A patch about 1/4 inch wider and longer than the gage was allowed for each gage.

(iii) All traces of grease and oil were removed from the specimen, using carbon tetrachloride. Care was taken to see that the fingers did not touch the prepared rock surface.

(iv) A final cleaning with Kleenex tissue and carbon tetrachloride was carried out so that the last traces of grease were removed. The specimen was then allowed to dry at room temperature until all obvious dampness was absent (about 2 minutes).

(v) The strain gages were then removed from the package, and special care was taken not to touch their under surface. If any grease or dampness reached this lower surface it was removed with carbon tetrachloride and fresh Kleenex.

(vi) A small amount of C. I. L. household cement was applied to the gage and the prepared area of the rock specimen.

(vii) The gage was pressed in place on the specimen, and all air bubbles were removed by rocking the thumb across the felt gage pad.

(viii) Precautions were taken to centre the gage, and to check its alignment in both the horizontal and vertical directions.

(ix) The specimen with its attached gage was then placed in a special drying press. A layer of thin cellophane paper was placed between the gage and the sponge rubber press plates, and the press was clamped shut.

(x) The cement was allowed to set for 24 hours with the specimen in the gage press. The specimen was then withdrawn and the cellophane removed. The specimen was allowed to dry for 48 hours at room temperature, thus ensuring positive gage setting.

(xi) Specimens that were not to be tested within the following 7 days were waterproofed with Cerisan wax or Ten-X compound before storage in sealed metal cans. Figure 13 shows the strain gage setting presses and the necessary supplies for applying strain gages to rock specimens. A group of specimens with attached gages is shown in Figure 14.

(xii) Before the actual physical testing of a rock specimen took place, the gage resistance was checked with an ohmmeter to ensure that all gages were functioning correctly. A minimum resistance of 100×10^6 ohms between the gage winding and the surface of the specimen was required for correct operation of the gage.

Testing Presses

The purpose of the press is to apply the necessary stress to the rock specimens. This stress must be applied uniformly to the specimen and remain constant during the period of observation. Two different presses were used in this test work, having been made available to the Mining Research Section by the Mineral Processing and the Physical Metallurgy divisions of the Mines Branch. An Amsler (hydraulic-type) testing machine, with ranges of 0-60, 000, 0-120, 000 and 0-600, 000 pounds load, was used for large specimens. As the lower 20% of the loading range is always considered inaccurate, this press was used only when the specimen diameter exceeded 1.75 inches (cross-sectional area of 2.4 sq in). For the smaller specimens, a Riehle (electronic-controlled mechanical-type) testing machine, with ranges of 0-3000, 0-6000, 0-12, 000, 0-30, 000 and 0-60, 000 pounds load, was used. Figures 15 and 16 show photographs of these two testing machines and the associated test apparatus.

When specimens of different cross-sectional areas are

Figure 13 - Strain gage presses and necessary supplies for applying strain gages to rock specimens.

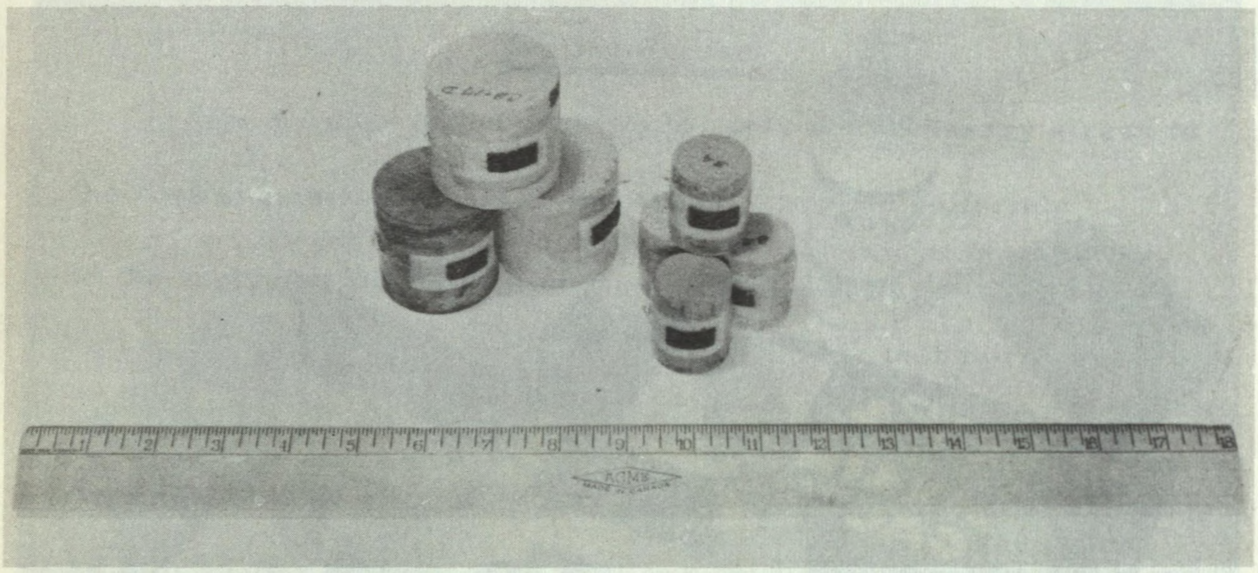

Figure 14 - A group of rock specimens with attached transverse strain gages.

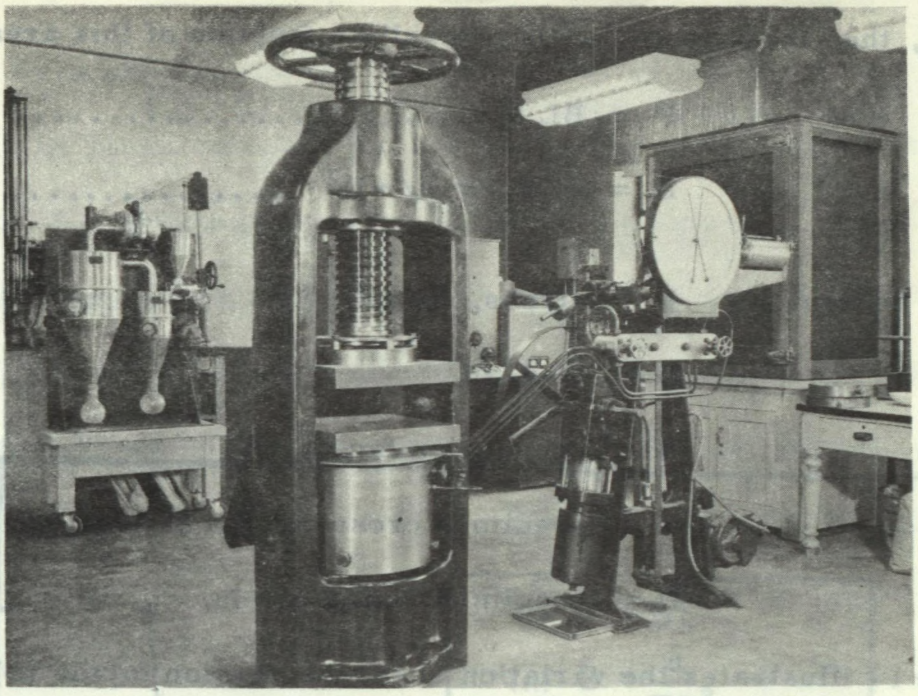

Figure 15 - Amsler hydraulic-type testing machine (Mineral Processing Division); capacity 600,000 lb.

Figure 16 - Riehle electromechanical-type testing machine (Physical Metallurgy Division); capacity, 60,000 lb.

tested, the stress in lb/in^2 is naturally a function of this area.

Now $$P = BL \qquad (35)$$

and $$B = 1/A = 4/\pi D^2 \qquad (36)$$

where P = stress, lb/in^2,

L = load, lb,

B = conversion factor,

A = specimen cross-sectional area, sq in, and

D = specimen diameter, in.

Figure 17 illustrates the variation of the conversion factor (B) with specimen diameter. Values of B for the commonly used specimen diameters are listed in Table 3.

TABLE 3

Variation of Cross Section and Conversion Factor with Specimen Diameter

Specimen Dimensions				Conversion Factor "B"
Diameter		Radius	Cross-section	1 lb Applied Load Converts to "B"
Inches		Inches	$(\text{Inches})^2$	(lb/in^2)
1/2	0.50	0.25	0.20	5.00
3/4	0.75	0.38	0.44	2.28
7/8	0.88	0.45	0.63	1.59
1	1.00	0.50	0.78	1.28
1-1/4	1.25	0.63	1.23	0.81
1-1/2	1.50	0.75	1.75	0.58
1-3/4	1.75	0.88	2.42	0.41
2	2.00	1.00	3.14	0.32
2-1/8	2.13	1.07	3.58	0.28
2-1/2	2.50	1.25	4.94	0.20
3	3.00	1.50	7.10	0.14

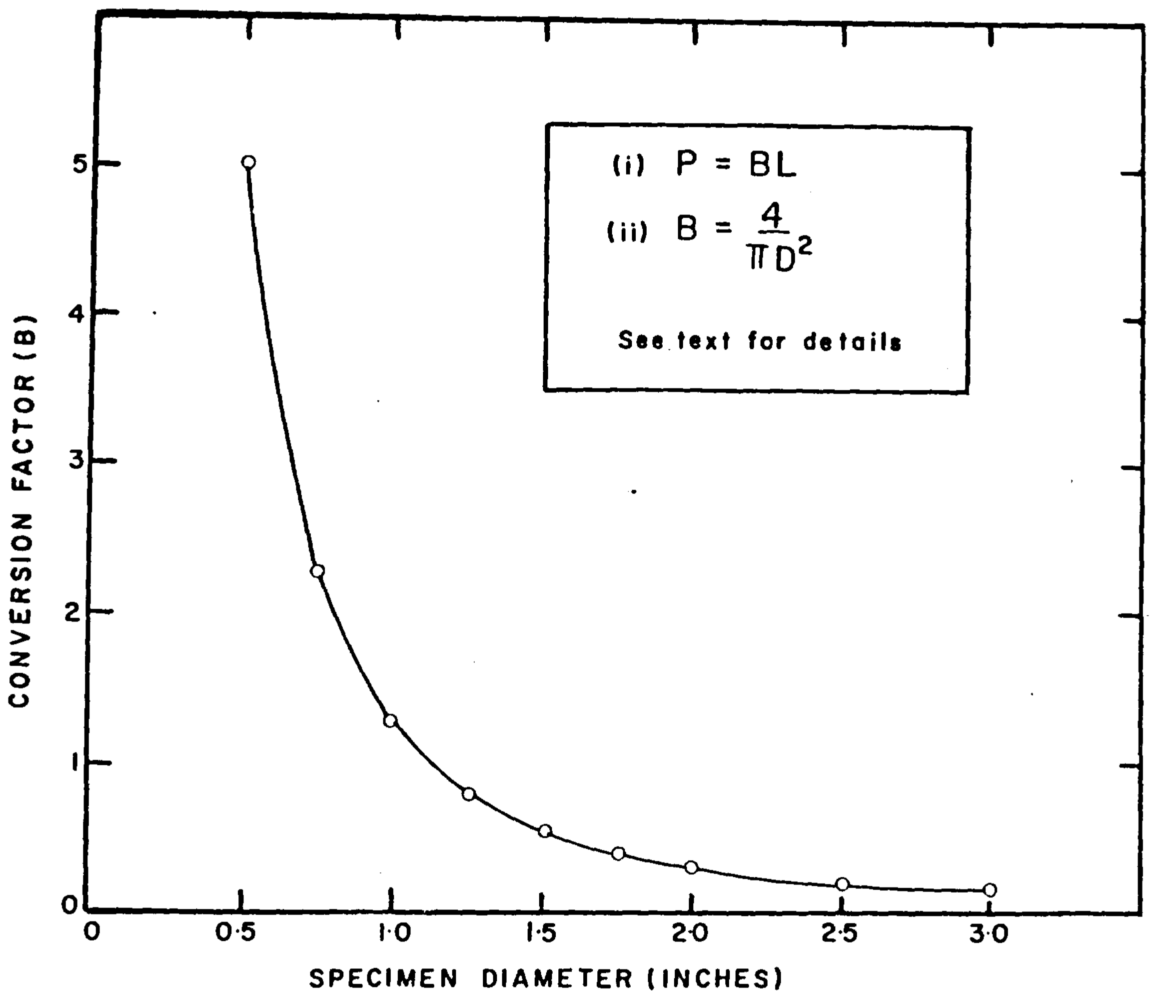

Figure 17 - Variation of specimen stress with diameter for fixed applied load.

ELASTIC AND FAILURE PROPERTIES

General

In the following sections the elastic and failure properties of mine rock specimens are carefully defined, the necessary calculations are discussed, and the experimental methods for their determination are described in detail.

First, the specimens were stressed over a loading cycle and the longitudinal and transverse strains were measured at each load increment. Stress-strain curves were plotted from these data, and from these curves the compression modulus and Poisson's ratio were obtained graphically. The specimens were then reloaded till failure took place. The ultimate compressive strength was determined from the load required to produce failure. The fracture angle and fracture classification were determined, and finally the strain energy was calculated.

Elastic Properties

Introduction

This section describes the complete test procedure for determining two of the elastic properties of rock specimens, namely compression modulus and Poisson's ratio, and includes definitions of terms, methods of calculation, and studies conducted to check the effect of such variables as specimen geometry, moisture and storage time on these elastic properties.

Very briefly, the test procedure was as follows:

The prepared specimen was cleaned and two A-5, SR-4 resistance-type strain gages were attached to measure transverse strain. These gages were aligned in such a way as to be sensitive only to changes in the circumference of the specimen. The specimen was then allowed to air-dry at room temperature for 48 hours,to permit the gage cement to set fully. For testing, the specimen was placed between two steel capping cylinders set between the plattens of a standard testing machine. The strain gage bridge was connected, and the Martens extensometer was attached to the capping cylinders. The Martens extensometer (mirror and telescope system) was adjusted, and zero load readings were obtained for both the Martens extensometer and the transverse strain gages. The stress was then increased through a loading cycle (0, 1, 2, 3, 4, 5, 6, 7, 8, 9, 10, 15, 20, 10, 5, 0 lb/ $in^2 \times 10^3$). At each value of applied stress the strain gage and Martens extensometer readings were observed. Longitudinal and transverse stress-strain curves were plotted from these observed data and, using a graphical method, values of compression modulus and Poisson's ratio were determined directly from these curves.

Compression Modulus

1. Definition

The definition of compression modulus as used in this particular study of mine rock characteristics should first be stated. Although this term is clearly defined when considering materials having linear stress-strain curves, it is not well defined for the type of material with which this report deals. For the purposes of this report the term 'compression modulus' is defined as "the value of Young's modulus in compression, as measured normal to the ends of a right-cylindrical rock specimen". For any material under stress, Young's modulus is defined [15] as "the applied stress divided by the resulting linear strain* produced in the direction of application of the stress".

Considering Figure 18, the value of compression modulus for the linear stress-strain curve OAB is simply the slope of the curve. It is also the ratio of the total stress OE to the total strain OD. There are, then, two distinct methods of measuring E_c (compression modulus), namely the tangent method and the total strain or secant method. In the case of a material having a linear stress-strain curve, the two methods would yield exactly the same results, but in the case of the non-linear stress-strain curve (OA'B') the secant method would yield a value of E_c of OE'/OD' and the tangent method would give a value of E_c which varied with the applied stress, since the slope of curve at A' differs greatly from the slope at B'. Results of many tests in the division's laboratories, [16] as well as of tests by other workers in this field, [17] have shown that non-linear stress-strain curves are followed by materials such as cements, rock and coal,

---

* Linear strain is defined as $\Delta L/L$, where L is the original length and ΔL is the change of length, and should not be confused with linearity of stress-strain curves.

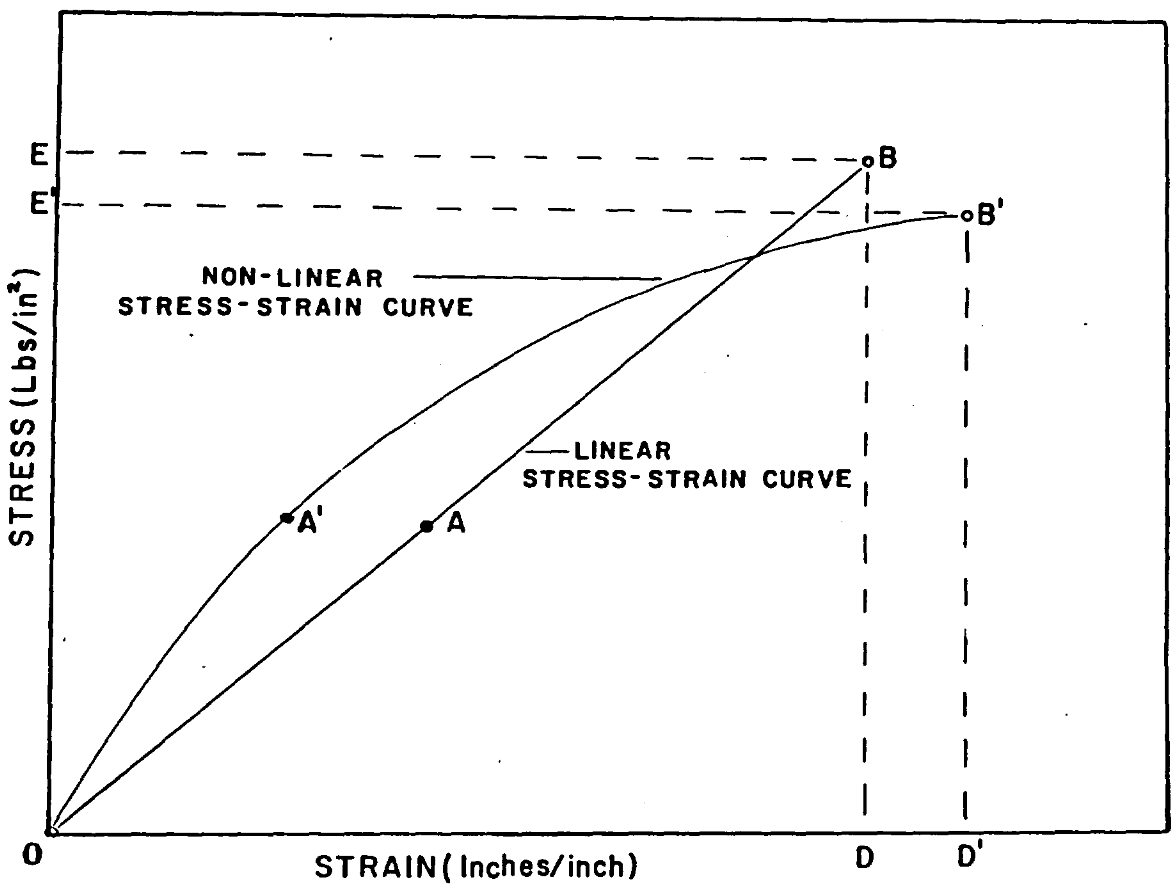

Figure 18 - Diagram illustrating linear and non-linear stress-strain curves.

thus resulting in the variation of elastic properties with applied stress as shown in Figures 19 and 20. It must be remembered, when setting up a group of experiments or tests of a comparative nature, that the compression modulus (as well as other elastic moduli) are functions of the applied stress as well as of the material. This would immediately rule out the use of compression modulus values found by the secant method, as these values are dependent on the shape of the whole stress-strain curve, whereas the compression modulus values found by the tangent method are dependent only on that portion of the curve under study.

As it was desired to compare the results of tests on all rock types, E_c was calculated at a value of 6×10^3 lb/in^2 stress, so that even the weak shales (which fail at about $6\text{-}8 \times 10^3$ lb/in^2) could be included. The value of E_c throughout this report is therefore defined to be, unless otherwise indicated, the slope of the tangent line drawn to the stress-strain curve at an applied stress of 6×10^3 lb/in^2

Considering the foregoing, the compression modulus is given by the following (see also Figure 25):

$$E_c = \Delta P / \Delta e_1 = W_p \ldots\ldots\ldots\ldots \quad (37)$$

where E_c = longitudinal compression modulus,

ΔP = increment of stress, and

Δe_1 = increment of longitudinal strain produced by ΔP.

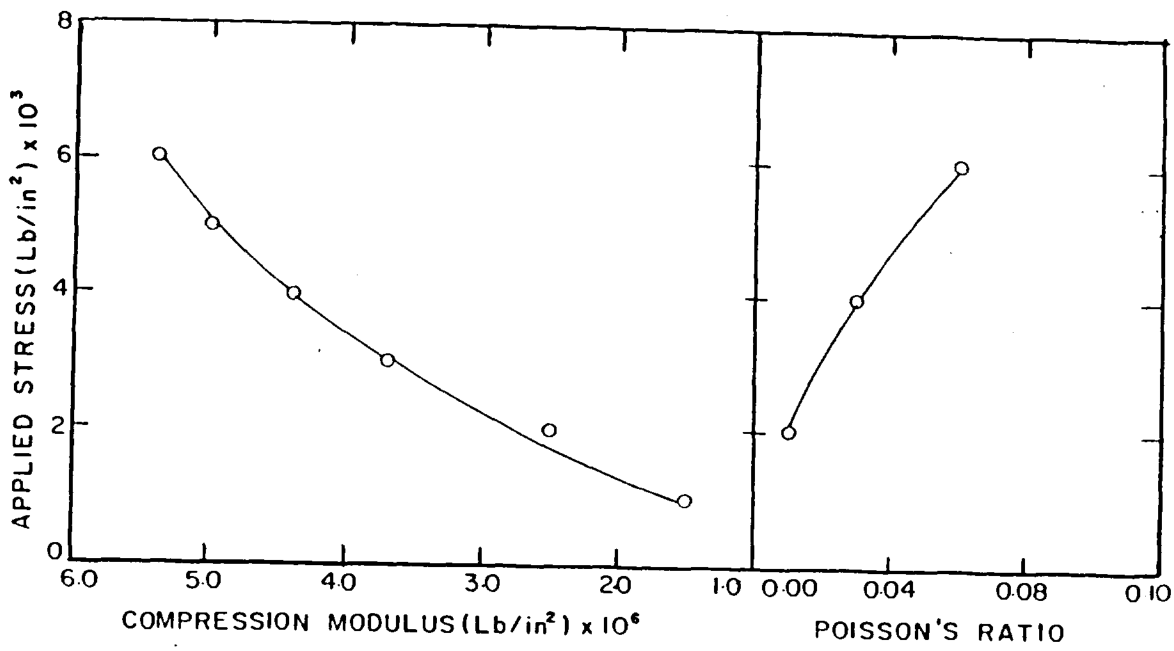

Figure 19 - Variation of elastic moduli with stress, for Springhill sandstone. (Test No. 743)

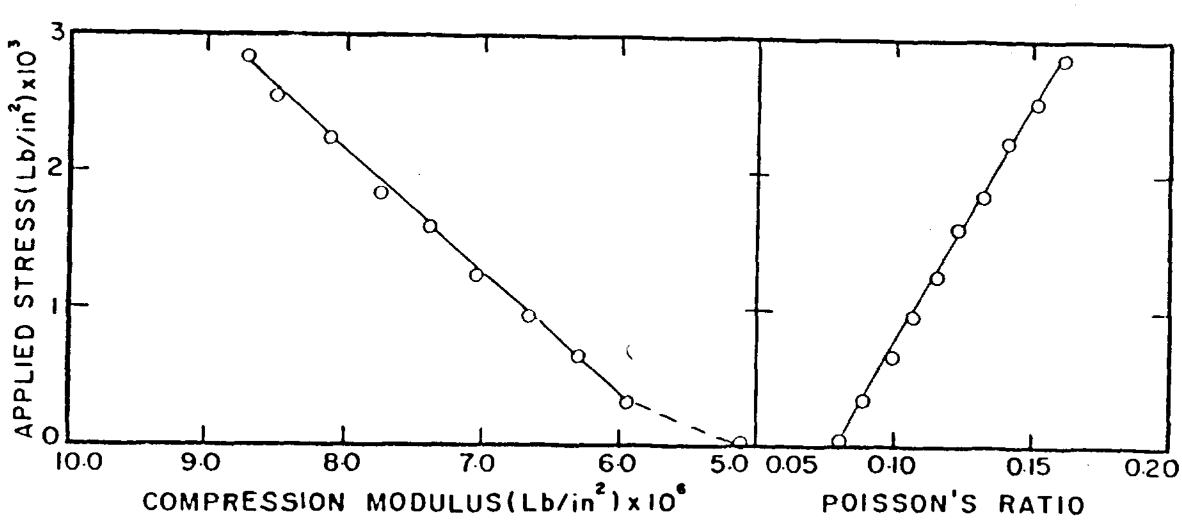

Figure 20 - Variation of elastic moduli with stress, for Rockport granite. (After Zisman)

W_p = slope of tangent line drawn to the longitudinal stress-strain curve at a stress of 6×10^3 lb/ in^2.

It should be noted that in an effort to reduce the number of calculations the compression modulus was determined by a graphical method, which is described in detail later (pp. 61-66) in this bulletin.

2. Correction for Capping Cylinders

Since the Martens extensometer was attached to steel capping cylinders at either end of the test specimen, the observed longitudinal strain was corrected, using equation (25), to give the true strain in the rock specimen.

3. Effect of Specimen Diameter

It has been shown by the U.S. Bureau of Mines [2] that the dynamic compression modulus (as determined by sonic tests) for materials such as rock is not dependent on specimen diameter. A few tests were carried out to check this result for the case of the static compression modulus (as determined by actual loading of the specimen). A set of three specimens, each with length 2.0 inches and diameter 2.14 inches, were selected for these tests. These were called the primary specimens. The primary specimens were first loaded in a hydraulic testing machine to 12.75×10^3 lb/ in^2 and the compression modulus determined by the secant method at that point. The specimens were then removed from the press and a 0.98 inch diameter core was drilled out of the centre of each primary specimen. The resultant outside and inside secondary specimens were then tested and the compression modulus at 12.75×10^3 lb/ in^2 determined again for each specimen. The test results are given in Table 4, and the dimensions of the primary and secondary specimens are shown in Figure 21.

TABLE 4

Variation of Compression Modulus* with Specimen Diameter

Specimen	Rock Type	E_c * (lb/ in^2) x 10^6	Average E_c (lb/ in^2) x 10^6	Percent Deviation
No. 1	Sandstone			
Primary		5.6	5.5	1
Sec - 1		5.3		-4
Sec - 2		5.7		3
No. 2	Sandstone			
Primary		6.8	6.9	-1
Sec - 1		6.9		1
Sec - 2		Broken		-
No. 3	Sandy Shale			
Primary		4.9	5.8	-15
Sec - 1		6.8		18
Sec - 2		5.6		3

* Compression modulus determined by the secant method.

In specimens 1 and 2, agreement was found in compression modulus obtained for the primary and secondary cores. However, in specimen 3 there was a lack of agreement. Considering only specimens 1 and 2, the variation in compression modulus with specimen diameter (from 1.0 - 2.2 inches) was less than 4.0%. It was concluded, therefore, that variation of specimen diameter in this range of

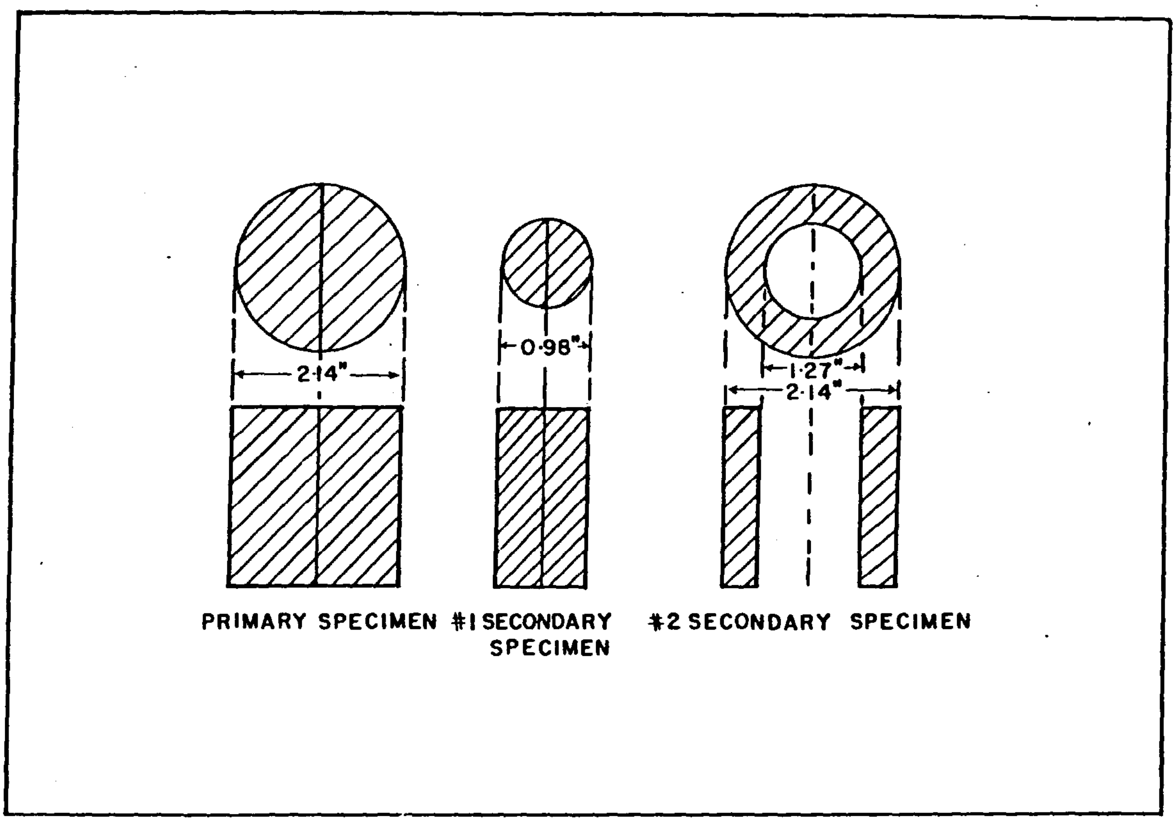

Figure 21 - Diagram illustrating dimensions of primary and secondary test specimens.

1.0-2.2 inches had little effect on the compression modulus determined by static testing.

4. Effect of Off-Centre Loading

A short series of tests was performed to observe the effect of off-centre loading on the experimentally determined value of compression modulus for a particular specimen. A 2.14 inch diameter specimen of sandstone was first loaded while centred in the testing machine. The strain was measured with increasing load, using the Martens extensometer, and the compression modulus determined by the secant method at 12.75×10^3 lb/ in^2. Next, the same specimen was moved off-centre 1/ 2 inch parallel to the extensometer knife edges, and again tested. Finally, the specimen was moved off-centre 1/2 inch toward the back extensometer knife edge and the test repeated. The results are shown in Table 5. Figure 22 illustrates the position of the specimen in relation to the centre of the press plate for the three tests.

TABLE 5

Variation of Experimentally Determined Compression Modulus with Specimen Position

Specimen Position	Experimentally Determined Compression Modulus (lb/ in^2) x 10^6	Deviation from Compression Modulus of Centred Specimen (lb/ in^2) x 10^6	Percent Deviation
1) Centred	7.1	-	-
2) Off- centre 1/2" to the right	6.0	1.1	15.5
3) Off- centre 1/2" to the back	6.3	0.8	11.3

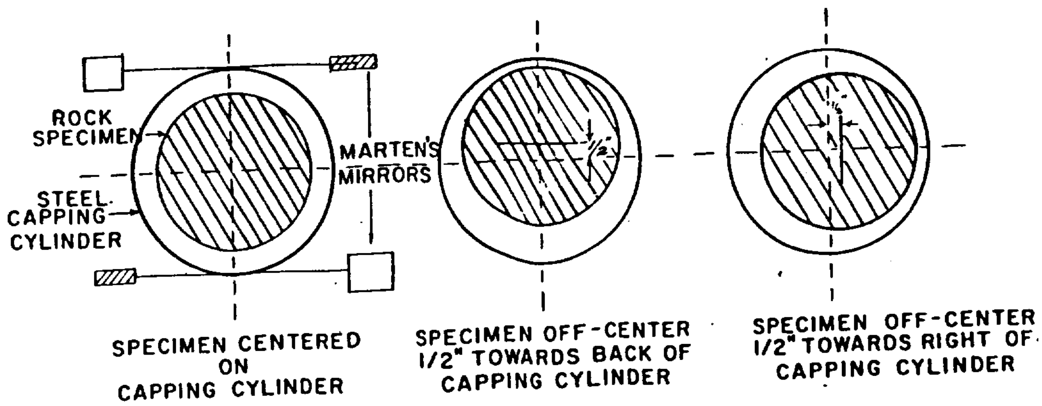

Figure 22 - Diagram illustrating different specimen positions for off-centre tests.

It was therefore concluded that with the Martens extensometer an error in centring the specimen of approximately 1/2 inch could result in an error of at least 10% in the compression modulus.

5. Effect of Moisture

It has been previously shown by the U.S. Bureau of Mines [2] that the presence of moisture in rock specimens greatly affects their elastic moduli. Figure 23 shows the variation of dynamic compression modulus with moisture content. However, the air-dried state was found by these workers to be a stable condition for test purposes. A standard drying period of 14 days (after preparation) at room temperature was considered ample. Reproducibility of test data was found to be good under these conditions.

6. Comparison of Compression Modulus Values Determined Using the Martens Extensometer and Strain Gages

In some particular instances* it was found more convenient to use SR-4 resistance-type strain gages, rather than the Martens extensometer, for measurement of longitudinal strain. So that all results would be comparable, a series of tests [18] was conducted to determine the relationship between the compression modulus as determined by the two test methods. A tentative correlation equation was obtained as follows:

$$E_1 = 0.3 + 0.68\, E_2 \pm 0.65 \qquad (38)$$

* At times, test work in the Ottawa laboratories was supplemented by work conducted at other locations where Martens apparatus was not available.

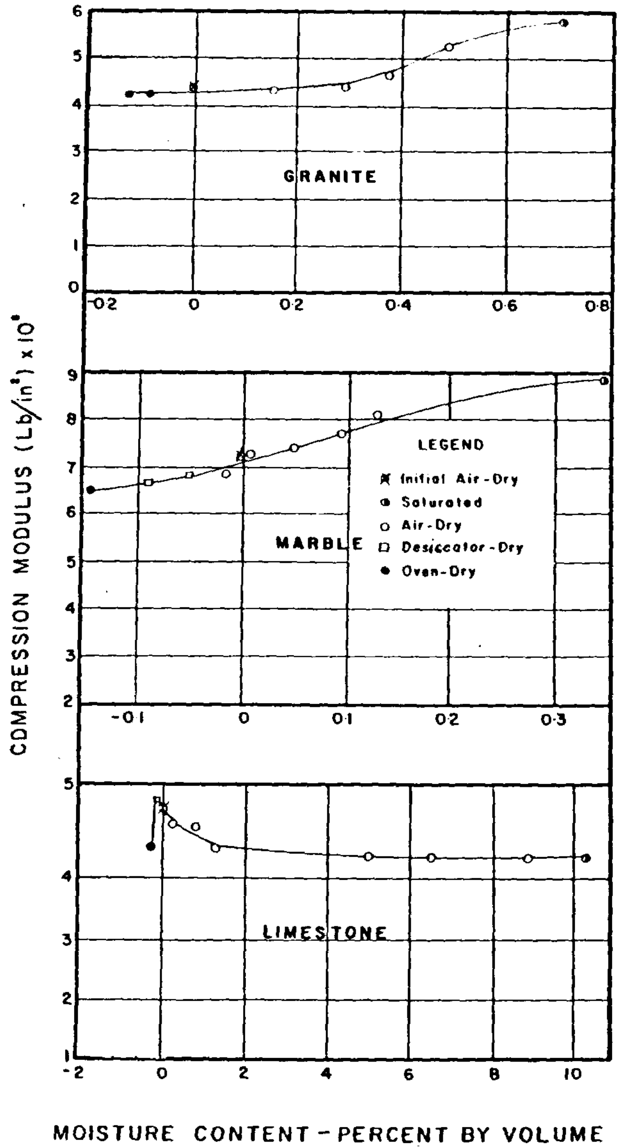

Figure 23 - Effect of moisture on compression modulus of mine rock. (After U.S. Bureau of Mines R.I. 3891)

where E_1 = compression modulus determined by Martens extensometer, and

E_2 = compression modulus determined by strain gages.

The fact that the results for one measuring system are not exactly equal to those obtained by the other is due to the limitations of the two methods, the strain gages being influenced by minor irregularities on the sides of the specimen whereas the Martens extensometer is affected by the presence of irregularities at the end faces of the specimen.

7. Daily Check of Test Procedure

To check on the stability of the test procedure from day to day (i.e. Martens extensometer, testing machine, and operators), a standard specimen of sandstone was selected and this specimen was tested a number of times over a three-month period. During these tests the specimen was loaded to 12.75×10^3 lb/ in^2 and the compression modulus was determined by the secant method at that point. These modulus values are illustrated graphically in Figure 24, and are listed in Table 6 along with the mean, standard deviation and percent standard deviation.

Although a few of the tests indicated large deviations from the mean (tests 7 and 9), the percent standard deviation for all the tests was only 6.1%, which was considered negligible for the purposes of this study.

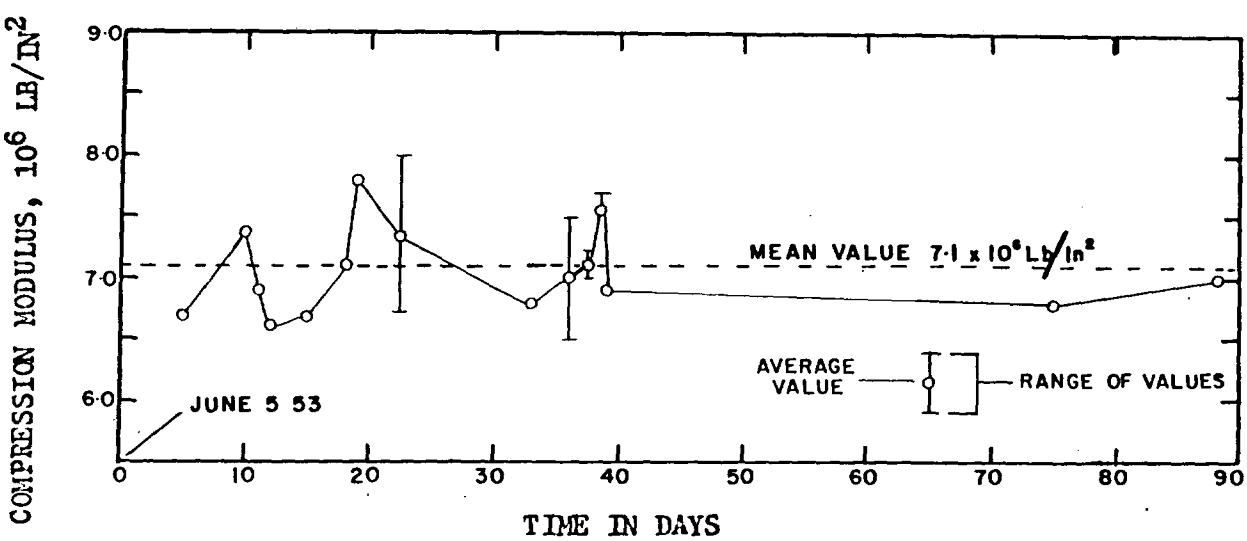

Figure 24 - Daily check of test procedure, showing variation of experimentally determined compression modulus for a number of tests on a single specimen.

TABLE 6

Daily Check on Test Procedure
(Summer, 1953)

Test Number	Date	Compression+ Modulus $(lb/in^2) \times 10^6$	Test Number	Date	Compression+ Modulus $(lb/in^2) \times 10^6$
1	June 5	6.7	11	July 3	6.7
2	" 10	7.4	12	" 6	7.5
3	" 11	6.9	13	" 6*	6.5
4	" 12	6.6	14	" 7	7.0
5	" 15	6.7	15	" 7*	7.2
6	" 18	7.1	16	" 8	7.4
7	" 19	7.8	17	" 8*	7.7
8	" 22	6.7	18	" 9	6.9
9	" 22*	8.0	19	Aug 14	6.8
10	July 3	6.8	20	Sept 7	7.0
Mean		7.1			
Standard Deviation		0.43			
% Standard Deviation		6.1%			

*Second test carried out at end of day.
+Determined by secant method at 12.75×10^3 lb/in^2.

8. Effect of Extended Storage

The effect of storage on the compression modulus of a group of 15 prepared specimens (all sandstone) was determined. The compression modulus was first determined during the summer of 1953, and then redetermined in the summer of 1955 after 24 months storage. The results of these tests are given in Table 7.

The average percent deviation from the original test values were -8.7% and +11.1%, and even larger values were noted, the maximum being +19%. However, assuming that each measurement of compression modulus is subject to a standard deviation of approximately 6% (see daily check of test procedure), and assuming that the

15 tests listed in Table 7 were conducted on similar material, then the results of the storage test are fairly consistent* with the results of the daily test. In this case, storage of the specimens does not appear to affect the compression modulus, at least not over a two-year period.

TABLE 7

Effect of Storage on Compression Modulus of Rock Specimens

Test Number	Compression Modulus (lb/in^2) x 10^6		Percent Deviation
	1953	1955	
361	4.4	4.2	-4.6
372	5.2	4.6	-11.5
381	4.5	4.2	-6.7
385	4.6	5.2	+13.0
388	4.6	5.3	+15.2
394	4.2	5.0	+19.0
397	5.3	4.8	-9.4
403	4.9	4.1	-14.3
408	3.5	4.0	+14.3
410	4.8	5.3	+10.4
413	5.5	5.1	-7.3
417	5.7	5.3	-7.3
420	4.5	4.7	+6.7
423	4.1	4.2	+2.4
426	4.5	4.9	+8.9

* The mean of the 15 tests conducted in 1953 was found to be 4.7 and, assuming a percent standard deviation of 6%, then the standard deviation would be 0.28. Theoretically, the difference between two measurements (1953 and 1955) should then have a standard deviation of $0.28\sqrt{2} = 0.4$. The standard deviation of the difference between measurements on the same specimen for the two test periods was actually found to be 0.53.

Poisson's Ratio

1. Definition

The usual definition of Poisson's ratio is as follows: If a uniform stress be applied to a specimen which is allowed to expand freely in all directions at right angles to the direction of the applied stress, the ratio of the linear* lateral (transverse) strain to the linear* longitudinal strain within the elastic limit of the material is defined as the Poisson's ratio.

In these studies cylindrical specimens were used, and, since the transverse or diametric strain in a cylinder is equal to the circumferential strain (see appendix B), the transverse strain was obtained by observing the resulting strain in the circumference of the specimen by means of attached resistance strain gages.

For materials, such as rock, which exhibit non-linear stress-strain curves, restrictions must be placed on the previous definition. It is necessary, as in the case of the longitudinal compression modulus, to state Poisson's ratio at a particular load (since the slope of the transverse as well as longitudinal stress-strain curves varies with stress). Considering the previous section, Poisson's ratio is defined by the following:

$$\mu = e_t/e_l \quad \ldots\ldots\ldots\ldots\ldots\ldots \quad (39)$$

where μ = Poisson's ratio,

*"Linear Strain" does not refer to linearity of stress-strain curves. (See foot-note page 42 under definition of compression modulus.)

e_t = transverse strain observed for applied load P, and

e_1 = longitudinal strain observed for applied load P.

However, this relation only holds true for linear longitudinal and transverse stress-strain curves. For a non-linear curve, Poisson's ratio is defined only over a small region, namely:

$$\mu = \Delta e_t / \Delta e_1 \qquad (40)$$

The following procedure was decided on for determining Poisson's ratio: The longitudinal and transverse strains were plotted against the stress applied during the loading cycle. Figure 25 shows the longitudinal strain curve OA'A and the transverse strain curve OB'B, plotted against applied stress. Previously, longitudinal compression modulus was defined as the slope of the tangent line drawn to the longitudinal stress-strain curve at a stress of 6×10^3 lb / in ^{2}. Now, arbitrarily, E_t is defined as equal to the slope of the tangent line drawn to the transverse stress-strain curve at the same value of stress.

Therefore $$E_t = \Delta P / \Delta e_t = B_p \qquad (41)$$

where ΔP = increment of stress,

Δe_t = increment of transverse strain produced by ΔP, and

B_p = slope of the tangent drawn to the transverse stress-strain curve at 6×10^3 lb / in ^{2}.

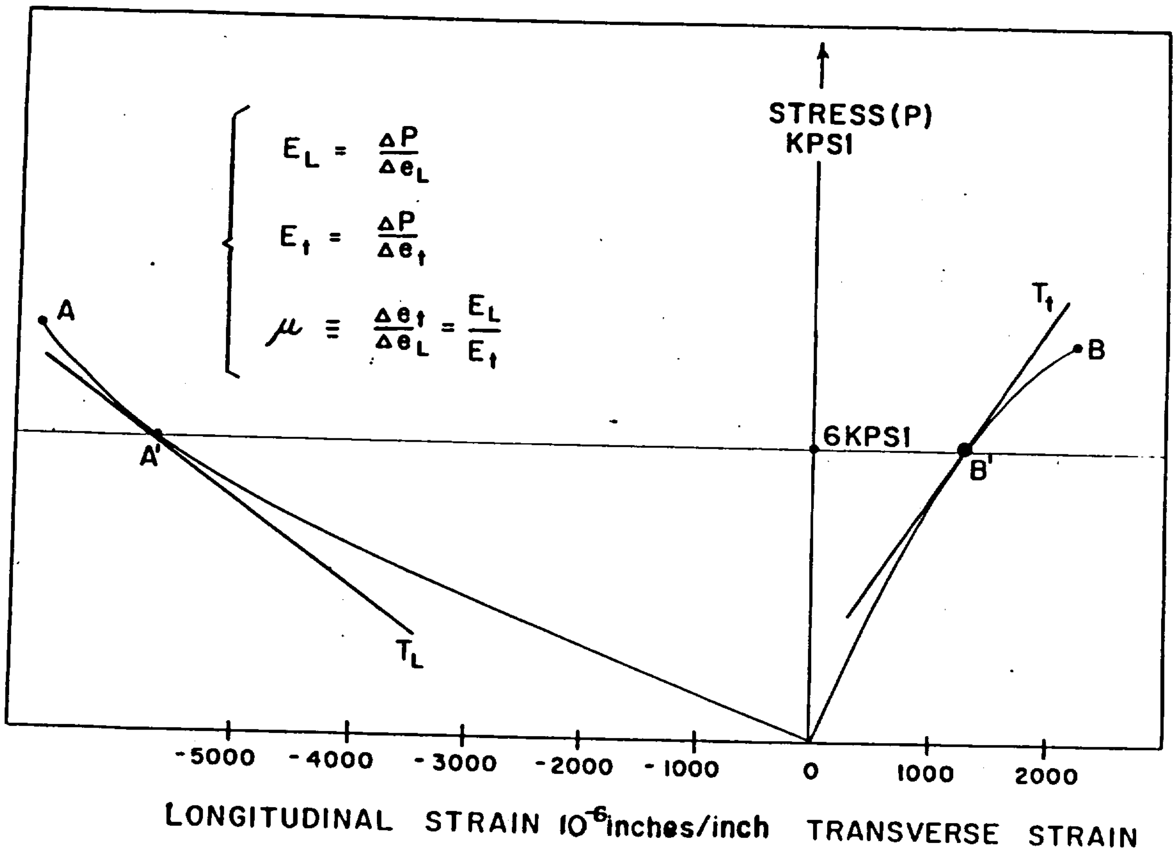

Figure 25 - Diagram illustrating graphical method of obtaining compression modulus and Poisson's ratio from stress-strain curves.

From (37) $\Delta e_1 = \Delta P / E_c$, and

from (41) $\Delta e_t = \Delta P / E_t$.

Substituting these into (40) gives:

$$\mu = E_c / E_t = W_p / B_p \quad \text{.................... (42)}$$

where W_p = slope of tangent line drawn to the longitudinal stress-strain curve at a stress of 6×10^3 lb / in ^{2}.

This relationship is particularly convenient for determining Poisson's ratio graphically.

Throughout this report, Poisson's ratio is determined at a stress of 6×10^3 lb / in. ^{2}, using equation (42) and the graphical method described later. It should be noted that if both the longitudinal and the transverse stress-strain curves are linear, Poisson's ratio reduces to the basic definition $(\mu = e_t / e_1)$.

2. Effect Due to Non-Linear Stress-Strain Curves and Other Factors

Since the values of E_c and E_t are determined by the tangent method at a specified value of stress, the effect of non-linearity of the stress-strain curves merely means that Poisson's ratio will be a function of the applied stress. The numerous factors affecting the compression modulus, described in previous sections, will therefore also apply directly to Poisson's ratio. It should also be noted that the experimental error incurred in determining Poisson's ratio will be necessarily larger than that for compression modulus, since it will depend on the experimental errors in both the longitudinal and transverse measurements.

Example showing Graphical Method of Obtaining
Compression Modulus and Poisson's Ratio

To simplify the determination of the compression modulus and Poisson's ratio, a standard plotting unit was designed and constructed. Figure 26 illustrates this unit, giving details of the strain plotting ruler, stress scale, and moduli protractors. One of the protractors was calibrated to read directly in longitudinal compression modulus and the other in (so-called) transverse compression modulus. Figure 27 shows a photograph of the completed plotting unit.

The theory behind the graphical method has been discussed in detail in the previous sections, but for a clearer understanding of the method the following example is included:

(a) Observed Data - The data given in Table 8 were taken from the test data obtained for a specimen of shale.*

(b) Initial Calculations - The only calculation that was necessary before plotting began was the addition of Columns 2 and 3, and the multiplication of the results by 1000 to convert them to strain (see equation (14)). These values were placed in column 4 as shown in Table 8.

* Barnsley Specimen #3A from the Broadsworth Mine, England.

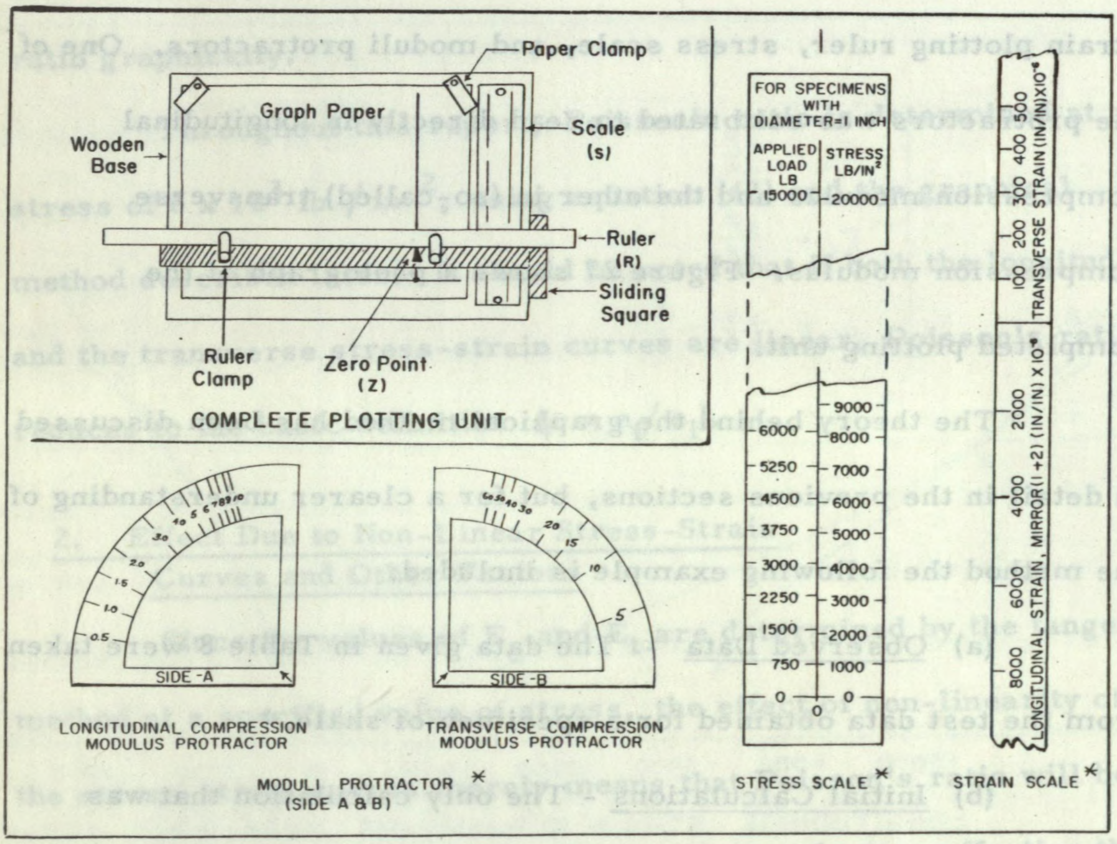

* These drawings are shown to scale   0   1"   2"

Figure 26 - Diagram illustrating details of stress-strain plotting units.

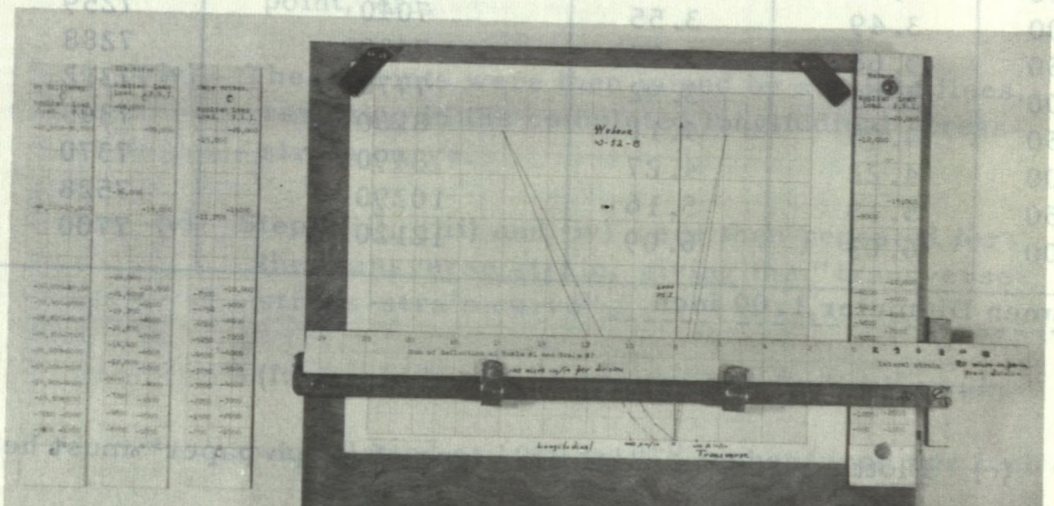

Figure 27 - Photograph of stress-strain plotting unit.

TABLE 8

Stress-Strain Test Data for Shale Specimen

Applied Load	Longitudinal Direction (Martens Mirror)			Transverse Direction (Strain Gages)
	Mirror - 1	Mirror - 2	Total-Mirror 1 and 2	
lb	Scale Reading	Scale Reading	(in/ in)x 10^{-6}	(in/ in)x 10^{-6}
0	1.88	1.67	3550	7109
750	2.32	2.32	4640	7129
1500	2.66	2.65	5310	7150
2250	2.90	2.93	5830	7178
3000	3.10	3.15	6250	7202
3750	3.30	3.37	6670	7230
4500	3.49	3.55	7040	7259
5250	3.68	3.75	7430	7288
6000	3.85	3.92	7770	7312
6750	4.05	4.11	8160	7345
7500	4.22	4.27	8490	7370
11250	5.13	5.16	10290	7528
15000	6.03	6.09	12120	7700

Specimen Diameter, 1.00 inch

(c) Plotting - One particular type of graph paper* must be used with this particular graphical unit. To use other types of paper, the scales and rulers would require recalibration. The steps in plotting were as follows:

(i) The proper load conversion scale was selected and fastened to the plotting board. The correct scale was selected according to the diameter of the test specimen (since its purpose

* Hughes Owens 315E-20 x 20, or any other make having 16 vertical and 20 horizontal major divisions, 1/2 inch in length, each subdivided into 10 equal parts.

is merely that of converting total specimen load to specimen stress in lb/ in^2). In this example the specimen diameter was 1.00 inch. The stress scale (vertical scale) for all specimens was the same regardless of specimen diameter, and only the total load scale varies.

(ii) The ruler (R) was set so that the no-load longitudinal strain (in this example 3550) fell at the zero point (Z). This point should correspond with the zero line on the graph paper.

(iii) The sliding square was shifted upwards over the paper until the ruler was parallel to the second load marking (750) on the stress scale (S). The appropriate longitudinal strain for this stress (4640) was marked on the graph paper. This process was continued for the third loading point, etc.

(iv) These points were then joined by straight lines, resulting in the completed longitudinal stress-strain curve.

(v) Steps (ii), (iii) and (iv) were then repeated for the transverse strain, giving the "transverse stress-strain curve".

(It should be noted that the longitudinal strain was plotted at 1000×10^{-6} inches/ inch per inch of graph, although the ruler was graduated at 2000×10^{-6} inches/ inch per inch of ruler. However, since the sum of the two strains (mirrors 1 and 2) actually being plotted was twice the average strain, this method results in the automatic averaging of the results from the two mirrors. The transverse strain, however, was plotted at a scale of 400×10^{-6} inches/ inch per inch of ruler on both the graph paper and the ruler.)

(vi) To measure compression modulus, the centre point of the protractor (Side A) was set at 6×10^3 lb/ in^2 on the longitudinal stress-strain curve, as shown in Figure 28, and with a clear plastic straight-edge the tangent to the curve at that point was obtained. The slope of this tangent was observed on the protractor, directly, in units of compression modulus. In this example a value of $E_c = 5.4 \times 10^6$ lb/ in^2 was obtained.

(vii) To obtain Poisson's ratio, the slope of the transverse stress-strain curve at 6×10^3 lb/ in^2 was obtained, using Side B of the protractor. In this example a value of 32×10^6 lb/ in^2 was observed. Then, using equation (42), Poisson's ratio was determined:

$$\mu = E_c / E_t = \frac{5.4 \times 10^6}{32 \times 10^6} = 0.17$$

(viii) The values of compression modulus and Poisson's ratio were then listed on the graph and on the test result sheets.

Standard Test Procedure for Determination of Elastic Properties

In accordance with the preceding sections, the following standard test procedure for the determination of compression modulus and Poisson's ratio was adopted:

(i) If possible, a sample long enough to produce three test specimens should be selected from each section of strata to be investigated. The prepared specimens should be free of obvious cracks or fractures, unless this is characteristic of the material, and should be 0.75 to 2.25 inches in diameter and at least 1.5 inches in length.

(ii) The specimens should be cut roughly to a right-cylindrical shape, using a diamond saw, and then ground accurately to the

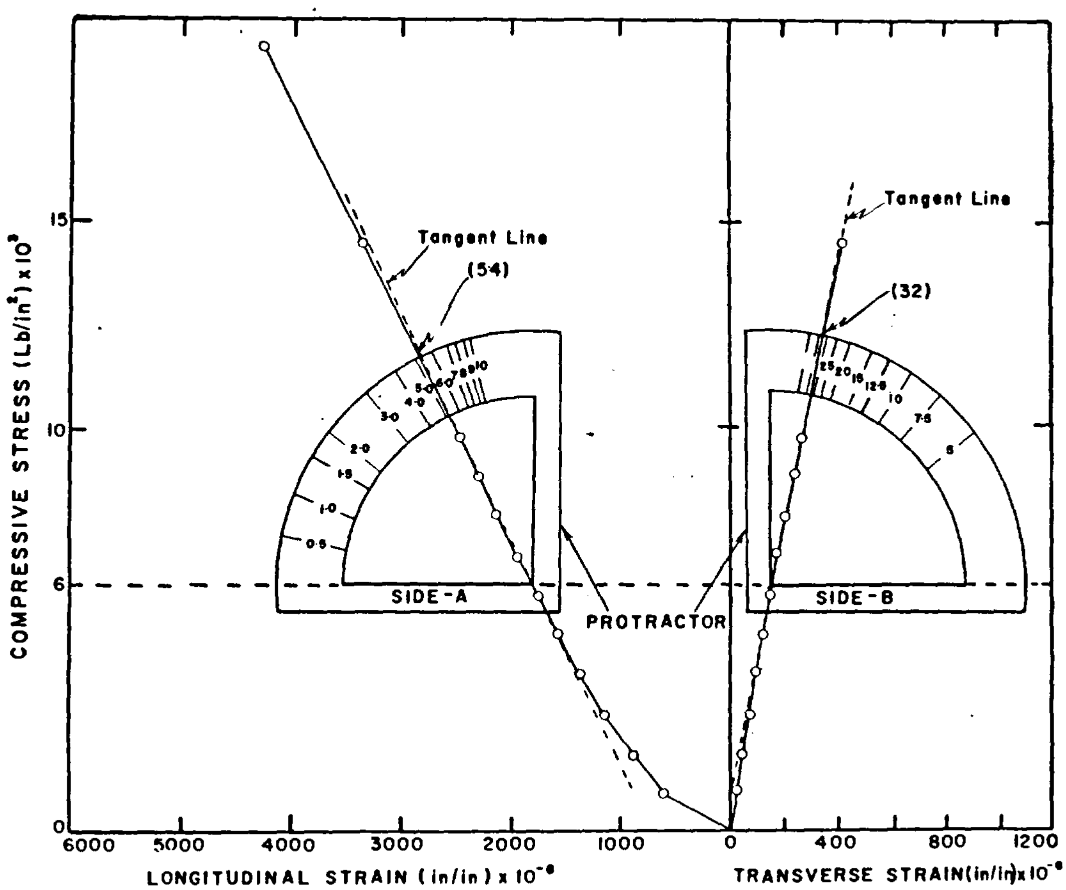

Figure 28 - Diagram illustrating method for obtaining compression modulus and Poisson's ratio directly from stress-strain curves, using moduli protractors.

proper length (following the standard preparation procedure), using a lap wheel and carborundum powder. A grinding jig should be employed to ensure that the ends of the specimen are "plane-parallel".

(iii) Following the preparation, the specimens should be allowed to air-dry at room temperature for 2 weeks. If the specimens are not to be tested immediately, they should be sealed in a metal container (to prevent change of moisture content) until the tests are to be carried out.

(iv) The diameter and length of the specimen are measured and the degree of parallelism of the ends determined. The specimen is weighed and its specific gravity calculated. These data are tabulated on the standard test data sheet a sample of which is shown in Figure 29.

(v) The two transverse SR-4 strain gages are attached to the specimens, which are then placed in the drying presses. Forty-eight hours should be allowed for the gage cement to harden properly.

(vi) The specimen, with its attached strain gages, is set between steel capping cylinders in the testing machine and the Martens extensometer is attached to these capping cylinders. The strain gage bridge is connected, and no-load (zero) readings are taken on both the strain gage bridge and the Martens extensometer.

(vii) The load is then cycled once over the path 0, 1, 2, 3, 4, 5, 6, 7, 8, 9, 10, 15, 20, 15, 10, 5, 0 $(lb/in^2) \times 10^3$. At each load point the values of longitudinal and transverse strain are observed and tabulated on the test data sheet.

(viii) The stress-strain curves are then plotted for both longitudinal and transverse strain. Following this, the compression modulus and Poisson's ratio are determined by the standard graphical method.

(ix) The calculated values of compression modulus and Poisson's ratio are then tabulated on a standard test result sheet, a sample of which is shown in Figure 30.

Fracture Properties

Introduction

The following section describes the complete test procedure

for determining four of the fracture properties of rock specimens,

TEST DATA SHEET

Mine ----------------------------- ________________

Specimen Lab. Number ------------- ________________

Specimen Length ------------------ ________________

Specimen Diameter ---------------- ________________

Rock Type - 1) Shale ☐ 2) sandy shale ☐ 3) sandstone ☐ 4) conglom. ☐ 5) ________ ☐

Grain Size - fine ☐ medium ☐ coarse ☐

Banding - no ☐ yes ☐ with 1 2 3 4 5

Visible Fractures - no ☐ yes ☐

COMPRESSION TEST

mirror to scale distance (Martens Mirror Extensometer) "a" = ________ inches
conversion factor (corresponding to above value of "a") "k" = ________

Applied load		Strain Longitudinal direction			Strain Transverse direction		
total	stress	mirror-1	mirror-2	average strain	gage-1	gage-2	average strain
Lbs.	Lbs/In^2	Rd'g	Rd'g	μ In/In	Defl'n	Defl'n	μ In/In

FRACTURE TEST

Total load at failure ________________ Lbs.

Compressive Strength ____________ Kpsi

Degree of Failure - violent ☐ noisy ☐ quiet ☐

Shape of Fracture - longitudinal ☐ diagonal ☐ cone ☐ (top ☐ bottom ☐) chunks ☐

Size of Remnants - small chips ☐ slices ☐ large pieces ☐

Figure 29 - Standard test data sheet.

TEST RESULT SHEET

Mine ----------- ____________________

Location ------- ____________________

Bore Hole ------ ____________________

Date Tested ------ ____________________

Technician ------- ____________________

Bore Hole Position	Test Number	Footage	Rock Type and Remarks	Grain Size	Hardness	Individual Values			Average Values			Fracture Classification		
						E_c	μ	P_u	E_c	μ	P_u	(i)	(ii)	(iii)

Figure 30 - Standard test result sheet.

namely ultimate compressive strength, fracture angle, fracture classification, and strain energy at failure, and includes the definition of terms, method of calculation, and studies conducted to check the effect of such variables as specimen geometry, moisture and rate of loading on these fracture properties. Very briefly, the test procedure was as follows:

The prepared specimens (previously prepared to study elastic properties) were centred in the testing machine between the spherically seated upper compression block and a fixed lower one. The initial load was applied slowly, to allow alignment of the spherical block. To protect the operator from rock fragments projected during failure, a heavy cloth was wrapped about the specimen. The load was then increased slowly at a constant rate until the specimen failed.

The ultimate compressive strength was determined from the load required to produce failure and from the geometry of the specimen. The fracture angle was measured and the fracture fragments were examined and classified. Finally, the strain energy at failure was calculated from the previously determined value of compression modulus and from the ultimate compressive strength.

<u>Ultimate Compressive Strength</u>

<u>1. Definition</u>

The ultimate compressive strength was defined as the stress required to induce failure in a cylindrical specimen with diameter and height equal, and in the absence of side constraint. Failure of the specimen was considered to have taken place when a sudden drop in applied load was observed and no further load could be supported.

The calculation of ultimate compressive strength for a cylindrical specimen with equal diameter and height follows directly from the definition above, namely:

$$P_u = L_f / A \quad \text{.........................} \quad (43)$$

where P_u = ultimate compressive strength, lb/in^2,

L_f = load required to produce failure, lb, and

A = cross-sectional area of the test specimen, sq in.

This equation applies to specimens of cylindrical and square prismatic shape, provided their length and diameter (or lateral dimensions) are equal. However, many bore hole core samples received from the field are of small diameter (0.75 - 1.50 inches), and as it is found impractical to use test specimens shorter than 1.50 inches, because of difficulty in attaching strain gages, the tests must be carried out on specimens with length considerably greater than diameter. In these cases equation (43) was replaced by one developed by the A.S.T.M. [19] for studies on natural building stone and later found by the U.S. Bureau of Mines [2] to hold for all rock types:

$$P_u = \frac{P_u'}{(0.778 + 0.222\, D/H)} \quad \text{..........} \quad (44)$$

where P_u = ultimate compressive strength of an equivalent specimen with D/H = 1.00, lb/in^2,

P_u' = apparent ultimate compressive strength of actual test specimen, lb/in^2,

D = diameter or lateral dimensions of specimen, in inches, and

H = length of specimen, in inches,

When D is less than H, P_u' is less than P_u owing to a tendency of the specimen to bend. Figure 31 shows the dependence of P_u/P_u' on D/H.

2. Effect of Specimen Length and Diameter

Aside from the effect of the D/H ratio, it has been shown previously (2) that variation of specimen diameter and/or length in the range 0.5 to 4.0 inches has little or no effect on the ultimate compressive strength.

3. Effect of Capping Material

It has been shown (2) that if capping material (for example, blotting paper) be placed between the test specimen and the compression blocks, the standard deviation of results will be slightly reduced. However, the average value of ultimate compressive strength will also be reduced. It was decided not to use any capping material in these tests.

4. Effect of Moisture

Tests conducted by other workers (2) indicate that the ultimate compressive strength of rock specimens increases with

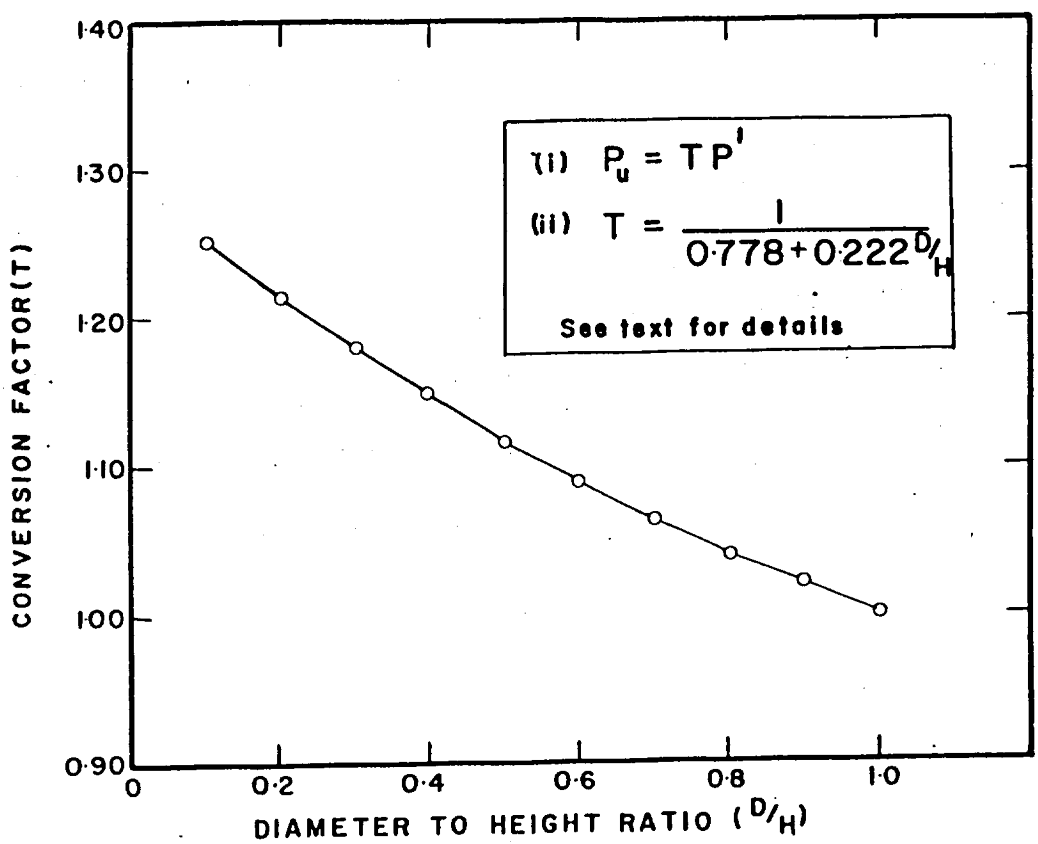

Figure 31 - Variation of calculated ultimate compressive strength with D/H ratio for experimentally determined values of failure stress.

decreasing and decreases with increasing moisture. The air-dried state was found to give the most reproducible results, and was selected by these workers as the standard. All specimens studied at the Fuels and Mining Practice Division were allowed to air-dry 14 days (after preparation) before testing.

5. Effect of Rate of Loading

It has also been shown[2] that there is no significant difference in ultimate compressive strength values determined by tests on specimens of similar material using different rates of loading (rates of 100, 200 and 400 lb $/ in^2$ per second were tried). A standard rate of loading of 200 lb $/ in^2$ per second was adopted for these studies.

Fracture Angle

In many cases the major remnants of the specimen after failure were found to be either conical or bounded by a plane of shear failure inclined to the axis of the original specimen, the latter type of failure being termed diagonal (see Figure 32). In the conical case, the apex angle α was measured and the fracture angle $\beta = \frac{\alpha}{2}$ was calculated. In the diagonal case, the fracture angle was determined directly as the minimum angle between the plane of failure and the side of the specimen. These angle data were then tabulated with the other test results. Figure 33 shows a number of photographs of fractured rock specimens.

According to Phillips[20], most coal measure rocks fail like brittle bodies even though time-strain (creep) is exhibited in most

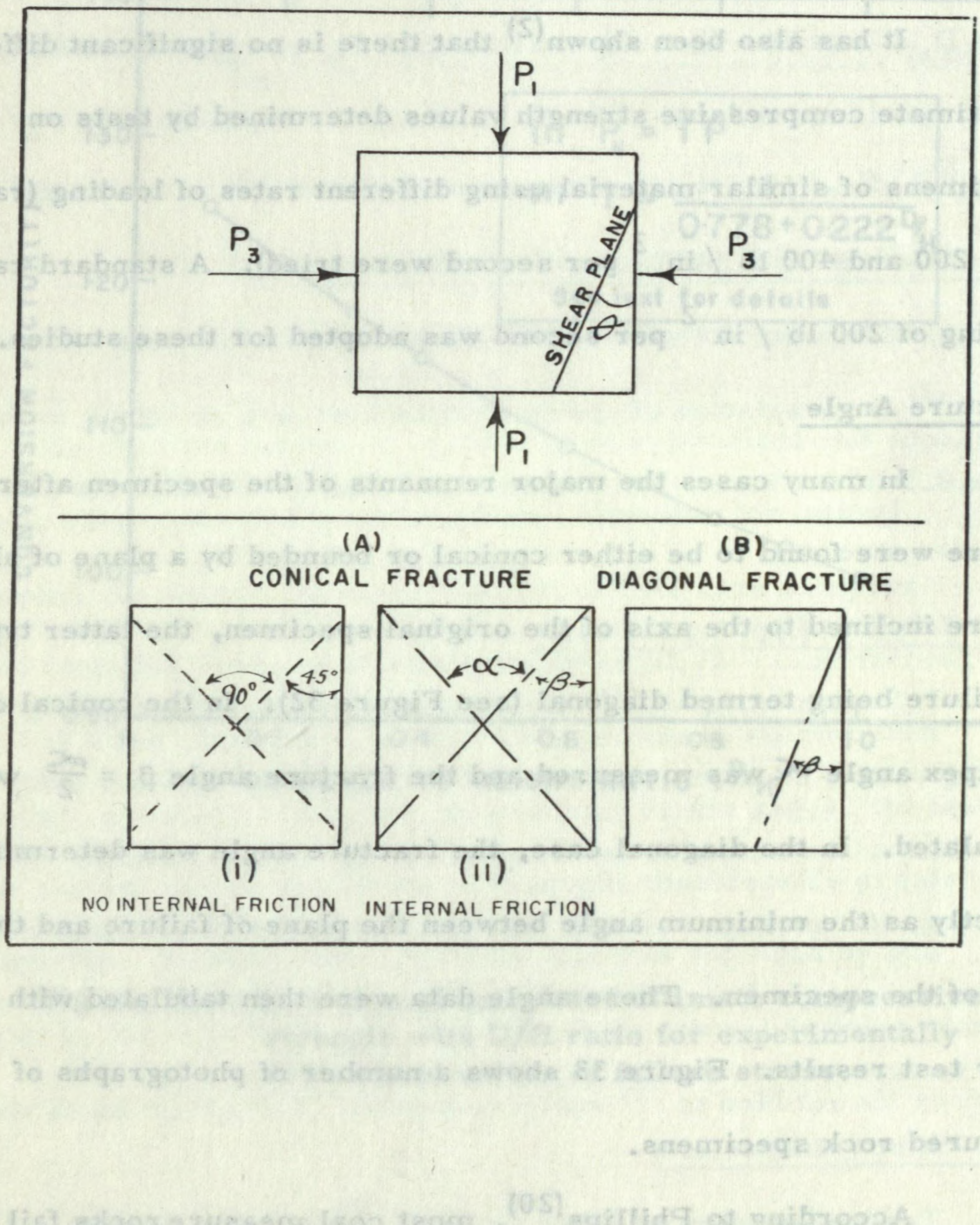

Figure 32 - Diagram illustrating the relationship of shear planes and principal stresses in a stressed body.

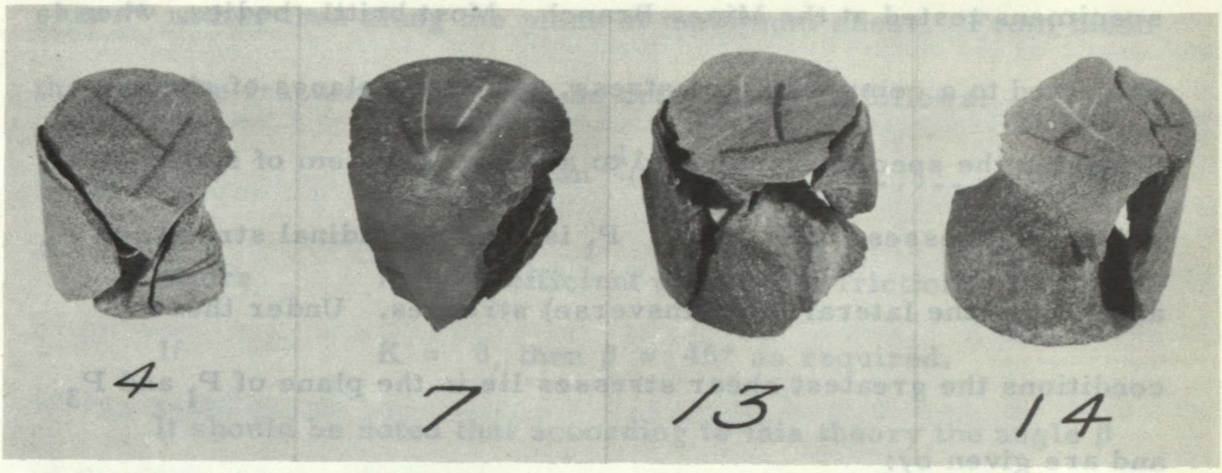

(A) Specimens labeled 4, 7, 13 and 14 are representative of conical fractures. Specimens 4 and 7 appear to be wedge shaped, whereas the base cones in 13 and 14 are better developed.

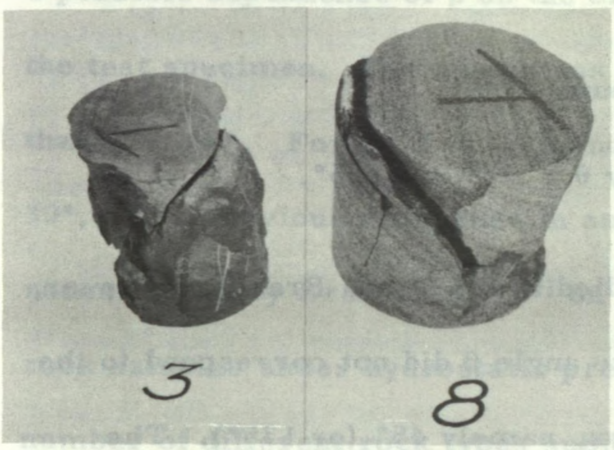

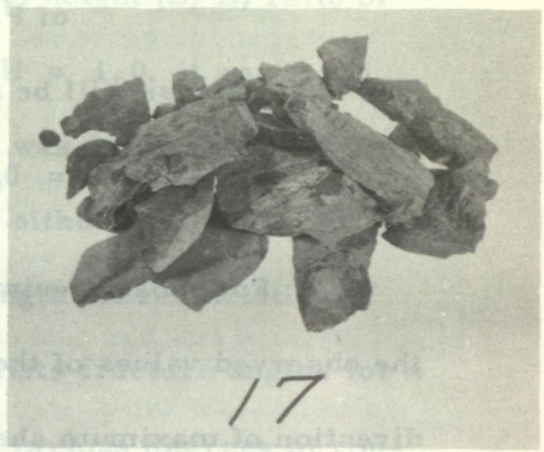

(B) Specimens 3 and 8 are representative of diagonal fractures. These appear well defined.

(C) Specimen 17 illustrates longitudinal fracture fragments.

Figure 33 - Photographs of fractured rock specimens, illustrating various modes of failure.

cases. This has been found to be the case with many of the specimens tested at the Mines Branch. Most brittle bodies, when subjected to a compressional stress, fail along planes of shear. Consider the specimen subjected to a triaxial system of stress with principal stresses $P_1 > P_2 > P_3$*. P_1 is the longitudinal stress and P_2 and P_3 are the lateral (or transverse) stresses. Under these conditions the greatest shear stresses lie in the plane of P_1 and P_3 and are given by:

$$S = \frac{1}{2} (P_1 - P_3) \sin 2\theta \quad \ldots\ldots\ldots\ldots\ldots\ldots \quad (45)$$

where S = shear stress acting on a plane whose normal lies in the plane of P_1 and P_3, and

θ = angle between shear plane and direction of P_1.

The shear stress will be a maximum

where $\frac{dS}{d\theta} = 0$, namely $\theta = 45°$ and $135°$.

For most specimens studied at the Mines Branch, however, the observed values of the fracture angle β did not correspond to the direction of maximum shear stress, namely 45° (or 135°). The majority of specimens had values well below 45°. This condition is explained by a theory, due to Coulomb(21) (and later Navier), which

---

* Actually the tests discussed in this report were performed under conditions of approximately uniaxial stress since $P \gg P_2$ or P_3; $P_1 \approx 10,000$ lb. and $P_2 = P_3 \approx 15$ lb. (atmospheric pressure). However, for completeness the P_2 and P_3 terms will be retained.

considers the influence of internal friction on the direction of fracture. This causes the material to fail along a plane of "most effective shear" rather then along the plane of maximum shear. From these theories the fracture angle may be determined as follows:

$$\beta = 0.5 \tan^{-1}(1/K) \quad \ldots\ldots\ldots\ldots\ldots\ldots \quad (46)$$

where K = coefficient of internal friction.

If $K = 0$, then $\beta = 45°$ as required.

It should be noted that according to this theory the angle β should be dependent on the specimen material and be independent of both the specimen geometry and the confining pressure (P_2, P_3). Recent experiments by Birch and Le Comte [22] on limestone indicate a possible dependence of β on the diameter-to-height (D/H) ratio of the test specimen. For specimens with $D/H = 1.0$, it was found that $\beta = 45°$. For $D/H = 0.5$ and 0.33 it was found that $20° < \beta < 30°$, with no obvious difference in angles for either value of D/H. A recent paper by Bredthauer, [23] on the strength characteristics of rock samples under hydrostatic pressure, lists fracture angles for a number of different rock types subjected to various degrees of confining pressure. From these results there appears to be some dependence of fracture angle on confining pressure. Since only a few tests were conducted on each rock type, no definite conclusions can be drawn.

Fracture Classification

A qualitative record was maintained for the mode of failure of each specimen. This included very approximate descriptions of, first, the degree of failure as indicated by the noise produced; second, the shape of the major fracture fragments; and third, the size distribution of the fragments. It was planned to attempt, at a future date, a correlation between this description and the ultimate compressive strength and/or the strain energy at failure.

To simplify this description, a standard code was evolved as follows:

Fracture Classification

(i) Degree	(ii) Shape	(iii) Fragment Size
1. very violent	a - top cone	A - dust
2. violent	b - bottom cone	B - 1/16" - 1/4"
3. semi-violent	c - double cone	C - 1/4" - 1/2"
4. quiet	d - longitudinal	D - larger than 1/2"
5. no data	e - diagonal	E - mixture
	f - irregular	F - no data
	g - no data	

For example, a specimen which failed very violently, leaving a double cone and a mixture of small and large fragments, would be coded as 1-c-E.

Strain Energy

1. Definition

Another physical property of mine rock which is of particular interest is its ability to store strain energy. The strain energy is defined as the sum of all the work done on a body during a compression or extension of that body.(1) When a rock specimen is compressed, work is done on the specimen; this work is stored as potential or strain energy in the material. If the specimen is truly elastic, this energy is completely dissipated during the unloading process, provided it takes place slowly. If, however, the specimen should fail suddenly while loaded, the potential energy suddenly becomes available to do external work (e. g., projection of fracture fragments, or production of sound and seismic waves). A knowledge of the magnitude of the strain energy stored in mine rock is therefore of the utmost importance.

Consider a unit volume of material to be subjected to a normal stress in one direction only, as indicated in Figure 34. The stress is allowed to increase slowly from zero to P, causing a strain e in the specimen. The resultant stress-strain curve for the material is of the general shape shown in Figure 34, and, since materials such as coal and rock are being considered, this curve is usually of a non-linear nature.[16] The shaded area under the curve 0b is the work done on the specimen, during compression, up to the point b. The total strain energy stored in the specimen at the point b is, therefore:

$$W = \int_0^{P_a} f\,(P)\,dP \ldots\ldots\ldots\ldots\ldots\ldots\ldots \quad (47)$$

where W = strain energy at stress P_a,

$f\,(P)$ = functional relationship between stress and strain, and

P = applied stress.

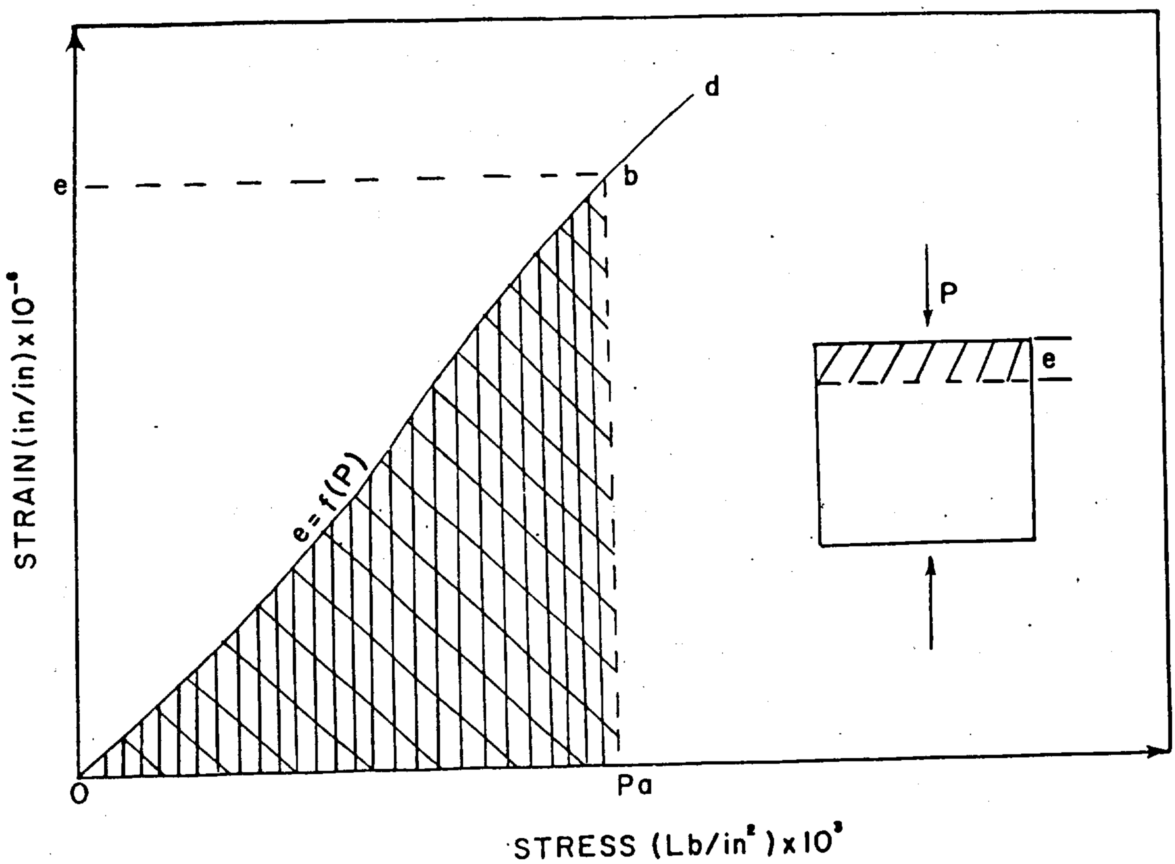

Figure 34 - Diagram illustrating the concept of elastic strain energy.

This integral may be calculated once the form of f(P) is known.

2. Calculation

The strain energy stored in a specimen under conditions of uniaxial stress with no lateral constraint may be derived as follows:

Assume the strain to be a linear function of stress, namely:

$$f(P) = P/E_c \quad \ldots\ldots\ldots\ldots\ldots\ldots\ldots\ldots (48)$$

where E_c = compression modulus.

Now substituting (48) into (47) gives:

$$W_a = \int_0^{Pa} f(P)\,dP = \frac{1}{E_c}\int_0^{Pa} P\,dP = \frac{1}{2E_c}\left[P^2\right]_0^{P_a}$$

and

$$W_a = \frac{1}{2} P_a^2/E_c \quad \ldots\ldots\ldots\ldots\ldots\ldots (49)$$

where P_a = stress at which strain energy is calculated.

The strain energy at failure is determined by setting $P_a = P_u$ (ultimate compressive strength), and is:

$$W_u = \frac{1}{2} P_u^2/E_c \quad \ldots\ldots\ldots\ldots\ldots\ldots\ldots (50)$$

Standard Test Procedure for Determination of Fracture Properties

After considering the preceding facts, the following standard test procedure was adopted for the determination of fracture properties:

(i) A group of three test specimens (usually the same specimens previously used to obtain the elastic properties) should be selected from each section of strata to be investigated. The specimens should be free from obvious fractures or planes of weakness, unless this is characteristic of the strata. Although they may have any convenient length and diameter, calculations are simplified if D/H = 1.00. Other specimen requirements are similar to those required when obtaining the elastic properties.

(ii) The specimens should be air-dried at room temperature for 14 days prior to testing. (This is only necessary when specimens have not been previously dried for other tests.)

(iii) The specimen is then placed in a standard testing machine, between an upper spherically seated compression block and a lower rigid one. An initial load of 200 lb/in^2 is first applied slowly to ensure proper alignment of the spherical block. A heavy cloth is wrapped around the specimen, to prevent the projection of rock fragments at failure.

(iv) The load is then increased on the specimen at a rate of 200 lb/in^2 per second until the specimen fails.

(v) The ultimate compressive strength of the material is calculated, using equation (43) or (44) depending on the value of the D/H ratio.

(vi) The fracture angle is determined and the fracture is classified according to degree, shape and fragment size. The data are recorded, using the standard code.

(vii) The calculated values of ultimate compressive strength and fracture classification are tabulated on the standard test result sheets shown in Figure 30.

(viii) The strain energy at failure is calculated from equation (50), using the value of ultimate compressive strength just determined and the values of compression modulus and Poisson's ratio, determined previously.

ANALYSIS OF TEST DATA

Introduction

After the specimens have been tested and their physical properties determined, using the methods and formulae described in the preceding sections, there remains the task of analysing these results. For each mine a large number of test specimens have been studied (200 is an average number) for some 10 physical properties, and consequently a great mass of data (approximately 2000 individual values) must be analysed to yield a group of representative quantities both for internal comparisons within a particular mine and for inter-mine comparisons. In spite of the large mass of data thus on hand, it was considered advisable to report all such data in order that other workers would be able to make their own statistical evaluations. To include only the author's interpreted values would have seriously reduced the value of the report. The physical properties of all specimens tested should be presented in tabular form as well as in the following two important reduced forms: first, graphs of the more important physical properties against distance (in the bore hole) from the seam, and second, distribution diagrams of a number of the more important properties.

The tables of results for individual specimens were used directly to prepare both the graphs and the distribution diagrams. These data will be invaluable for future statistical studies of rock characteristics. The graphs of physical properties of individual test specimens against position in the bore hole give a rapid and visual insight into the variation of the physical properties of the rock in relation to the seam. Finally, the data presented in the form of distribution diagrams immediately point out the mode and spread of the physical properties for each type. The mean, the standard deviation and the percent standard deviation, calculated from these distribution data, will be employed for inter-mine comparisons.

To check the quality of the results for each rock type, significance tests were carried out to determine whether the mean values for different rock types were significantly different.

Variation of Physical Properties with Distance from the Mineral Seam

Tabulation of Results

All physical properties determined in the preceding tests are listed in tabular form. Separate tables are established for each bore hole, and the data are arranged in order of position of the test specimen with respect to the mineral seam. Table 9, for example, shows the tabulated data for a bore hole (No. 12) at the McGillivray mine, Coleman, Alberta.[24] All physical properties that were determined are listed for each test specimen. Although the presentation of data for all test specimens increases the work required in producing a final report, it is considered justified, since this provides the basic data for any future calculations or statistical analyses which might be required.

TABLE 9

Tabulated Data for Bore Hole No. 12, McGillivray Mine, Coleman, Alberta.

Bore Hole Position	Test No.	Footage (Ft, In) Start	End	Strata Group	Specimen Description Rock Type	Remarks	Grain Size (1)	Apparent Specific Gravity	Mohs Hardness	E_c(3) $(Lb/in^2)x10^6$	Pu(3) $(Lb/in^2)x10^3$	μ (3)	W(3) In-Lb / in^3	Fracture Data (2)	β (3) Degrees
1	497	2,0	2,4	12-1	Shale	-	N.C.	-	2	4.4	22.5	0.07	57	2-c-F	-
2	498	28,0	28,4	12-2	Shale	-	N.C.	-	3	3.7	20.4	0.08	56	2-c-F	-
3	499	35,0	35,4	12-2	Sandstone	-	M.G.	-	3-4	1.7	11.8	-	41	4-d-F	-
4	1400	45,0	45,4	12-2	Sandy Shale	-	N.C.	-	3-4	3.4	24.7	0.05	90	2-g-F	-
5 (a)	1401	70,0	70,6	12-3	Sandstone	-	M.G.	-	3-4	3.0	20.6	0.08	71	2-c-F	-
(b)	1402	"	"	"	"	-	M.G.	-	-	1.9	12.3	-	38	4-d-F	-

SUMMARY OF SYMBOLS USED IN TABLE

(1) Grain Size Classification

F.G. - fine grain (up to 0.2 mm in diameter)

M.G. - medium grain (up to 0.5 mm in diameter)

C.G. - coarse grain (up to 0.8 mm in diameter)

N.C. - not classified

(2) Fracture Classification

(i) Degree
1 - very violent
2 - violent
3 - semi-violent
4 - quiet
5 - no data

(ii) Shape
a - top cone
b - bottom cone
c - double cone
d - longitudinal
e - diagonal
f - irregular
g - no data

(iii) Fragment Size
A - dust
B - 1/16" - 1/4"
C - 1/4" - 1/2"
D - larger than 1/2"
E - mixture
F - no data

(3) Summary of Symbols and Units

Symbol	Property	Units
Ec*	compression modulus	$(Lb/in^2)x10^6$
Pu	ultimate compressive strength	$(Lb/in^2)x10^3$
μ*	Poisson's ratio	---
W	strain energy (at failure)	$In\text{-}Lb/in^3$
β	fracture angle	Degrees

* Values of Ec and μ determined from stress-strain curves at 6×10^3 Lb/in^2.

Variation of Physical Properties over Small Vertical Distances (1-10 Inches)

From previous test data it was observed that the physical properties of one particular rock type varied greatly from one bed to another. However, closer inspection of the data showed that large variations in the physical properties were also evident, even in adjacent specimens selected from the same rock bed. A series of tests was performed in an attempt to observe this variation and to determine whether or not it was of a random nature. Briefly, the procedure was as follows: two pieces of rock core (about 12" in length) were obtained from what appeared to be two homogeneous rock beds. In each case, five adjacent specimens (2" in length) were removed from each piece of core. These ten rock specimens were then tested by the method developed in this report, and values of compression modulus and ultimate compressive strength were obtained for each specimen. The results are given in Table 10 and shown graphically in Figure 35. In both groups of test specimens an obvious change in physical characteristics was observed over the 12 inch length of core sampled.

The large variation in the physical properties of a number of different rock specimens from a single bed indicates that it would be incorrect to consider one specimen from that bed as representative of the whole. It should also be noted that, although the specimens in Groups 1 and 2 show a fairly continuous variation of physical

TABLE 10

Variation of Compression Modulus and Ultimate Compressive Strength of Rock Specimens over Small Vertical Distances

		Test No.	Compression Modulus+ $(lb/in^2) \times 10^6$	% Dev'n from Mean	Ultimate Compressive Strength $(lb/in^2) \times 10^3$	% Dev'n from Mean
Group No. 1 (*)	1	747	3.0	-9.1%	26.8	-16.2%
	2	748	3.1	-6.1%	26.8	-16.2%
	3	749	3.4	3.0%	32.8	2.5%
	4	750	3.5	6.1%	36.8	15.0%
	5	751	3.7	12.0%	38.0	18.7%
		Mean	3.3		32.0	
Group No. 2(**)	1	223	5.6	-8.2%	22.7	30.0%
	2	224	5.8	-4.9%	-	-
	3	225	6.3	3.3%	39.8	21.7%
	4	226	6.5	6.5%	24.8	-24.0%
	5	227	6.5	6.5%	43.4	33.0%
		Mean	6.1		32.7	

\+ Secant value at 6×10^3 lb/in^2 stress.
* Specimens from Springhill, Nova Scotia.
** Specimens from International Mine, Coleman, Alberta.

characteristics with distance, many similar groups of three or four adjacent specimens, tested in the Mining Section, showed very random variation in the same physical characteristics. Both conditions, i. e. the random and the continuous variation of the physical characteristics of a group of specimens selected within inches of each other, suggest just how variable and heterogeneous is the material under study. As it is impossible to sample every inch of a particular rock seam, it was decided to select (if possible) three specimens, constituting

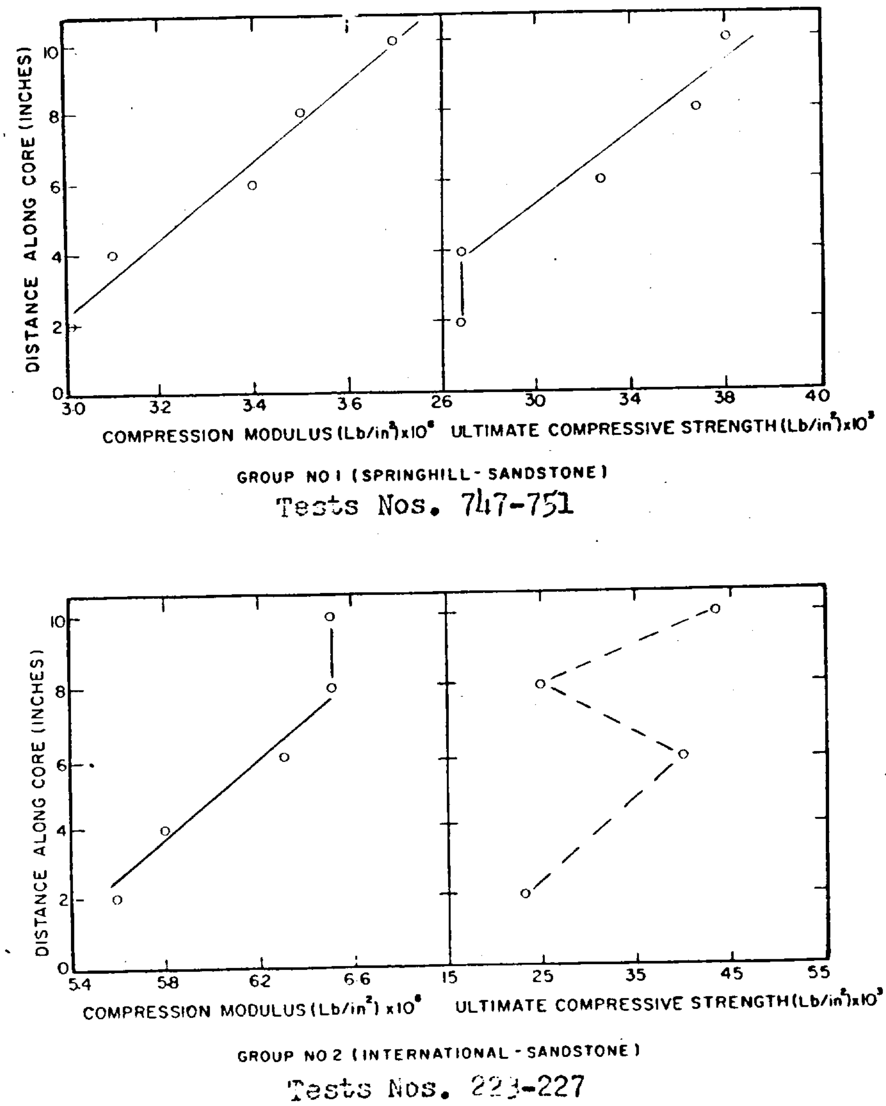

Figure 35 - Variation of compression modulus and ultimate compressive strength of two sets of rock specimens selected over small vertical distances.

a test set, at each sampling point.

The problem of averaging the values of a particular physical property for a test set under conditions of wide random variation in the values of the individual specimens is being considered.

Variation of Physical Properties Over Large Vertical Distances (1-100 Feet)

The variation of a number of the physical properties, namely compression modulus, Poisson's ratio, ultimate compressive strength, and strain energy at failure, are illustrated graphically so that variation with distance along the bore hole may be easily observed. For this purpose the average of each test set is plotted against the distance from the seam, different markings on the graph being used for each rock type. Figure 36 shows this variation in physical properties for the data listed in Table 9.

This was considered the most convenient method of displaying the variation of physical properties for different depths above or below the seam. The complete analysis for any mine should include such graphs for each bore hole studied.

Distribution Diagrams

Introduction

It must be understood that this analysis is not considered to be a perfect statistical picture of the results, for three important objections to its absolute validity arise. First, statistical evaluation

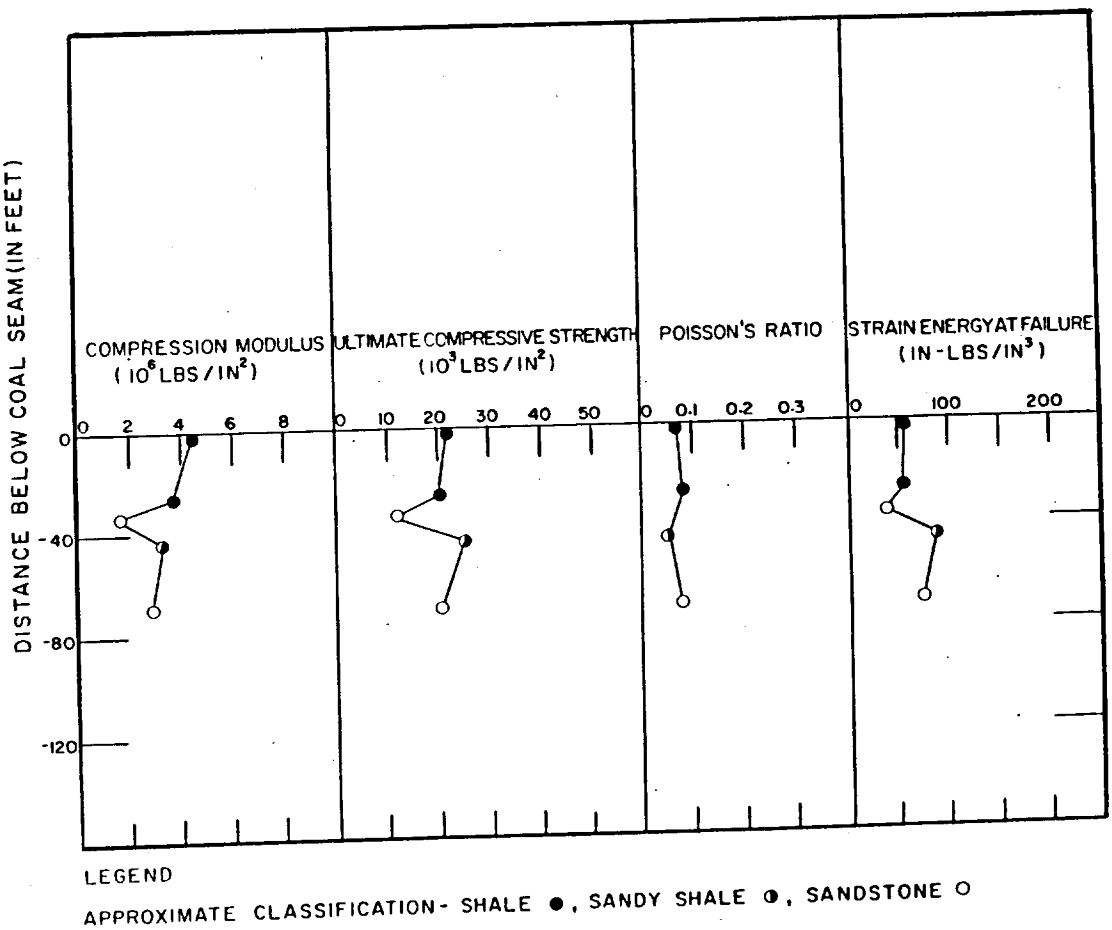

Figure 36 - Variation in average values of physical properties of mine rock over large vertical distances. (Bore Hole No. 12, McGillivray mine, Coleman, Alberta)

requires a random sampling which was not strictly adhered to in this case, for the test specimens were taken at intervals of approximately 10 - 12 inches along the drill core, and also at all points where there was a definite change in the type of strata. If a thick bed of one rock type exists, it is obvious that more specimens will be taken from this rock layer than from a thinner one. As a result the distribution diagram will be somewhat distorted. Secondly, the number of specimens tested is limited by time and the manpower available, and it will be appreciated that for a good statistical analysis many thousands of specimens may be required. Finally, the problem of classification of rock type, which is often found difficult,(11) may also tend to distort the distribution diagram. It is usually a simple matter to differentiate between a pure sandstone and a soft black shale, but the classification of the intermediate rocks (i.e. shaley sandstone, sandy shale, etc) is very difficult. It is the writer's opinion that a useful classification can only be made if a chemical and a microscopic analysis are done on each specimen tested, or if new primary standards of classification based on controlled scratch hardness or rebound hardness are adopted. A program of thin-section photography and chemical analysis, as well as hardness studies, is planned for the future.

The above three factors tend to produce distorted distribution diagrams. Therefore, great care must be taken to treat these diagrams with caution, always remembering that they are meant to show trends and limits and are not intended to express an exact mathematical function.

When considering the results of a particular test on a number of specimens, it is convenient to separate the total range of variation of the particular variable into intervals. The number of specimens per interval is then plotted against that interval, giving a diagram which indicates the distribution of that variable for a number of tests, each on a different specimen. In the case where repeated tests are being performed on the same specimen, the distribution curve would represent the range and magnitude of the experimental error. If (as in this work) a series of tests is conducted, each on a separate specimen of the same type of material (i.e. shale, sandstone, etc.), then the resulting curve would represent the expected range of variation for a particular physical property (for that material), as well as the range in which one would expect to find a certain percentage of the test results. The rock test data from all mines investigated were analysed in the same way. To illustrate the general procedure involved, test data from the McGillivray mine [24] were used.

Preparation of Distribution Diagrams

Distribution diagrams are generally prepared for the following properties: compression modulus, ultimate compressive strength, Poisson's ratio, strain energy at failure, and fracture angle, the distribution interval for these being 0.4×10^6 lb/in^2, 4.5×10^3 lb/in^2, 0.04, 29 in-lb/in^3 and 4 degrees respectively.

These intervals are, in general, of the same order of magnitude as the experimental errors in the different properties. As an example of the manner in which the distribution data are tabulated, the results for compression modulus for McGillivray mine rock [24] are shown in Table 11. Figure 37 shows these distribution data plotted in the standard form. A similar technique is used for tabulation and graphing of the data for the other properties, the only difference being in the value of the distribution interval. In all cases the scale of the ordinate (number of specimens in any interval) is adjusted to a convenient value to fit the distribution data.

Determination of Mode, Mean, Standard Deviation and Percent Standard Deviation

The following is a short review of the necessary statistical theory [25] used in the calculation of the final values of the experimentally determined physical characteristics.

Mode - The mode is defined as the value of the principal maximum of the distribution diagram. Values of the mode are normally indicated on the distribution diagram. Figure 37 shows four examples.

Mean - The mean (or average) of a number of values is determined as follows:

Consider a set of values

$$X1,\ X2,\ X3,\ \ldots\ldots\ldots\ldots\ldots\ldots\ \ Xn$$

The average for these n values is given by:

$$\text{Average} = \overline{X} = \frac{X1 + X2 + \ldots\ldots\ldots + Xn}{n}$$

TABLE 11

Tabulated Data for Compression Modulus Distribution Diagrams
(McGillivray Mine, Coleman, Alberta)

Compression Modulus Interval	Number of Specimens per Interval			
	Rock Type			
$(lb / in^2) \times 10^6$	Shale	Sandy Shale	Sandstone	Conglomerate
0.0-0.4	0	0	0	0
0.5-0.9	0	0	0	0
1.0-1.4	0	0	2	0
1.5-1.9	1	0	1	0
2.0-2.4	0	1	7	0
2.5-2.9	3	1	5	2
3.0-3.4	5	2	10	1
3.5-3.9	6	1	20	0
4.0-4.4	8	0	34	1
4.5-4.9	9	1	39	0
5.0-5.4	1	0	18	1
5.5-5.9	0	0	15	0
6.0-6.4	0	0	2	0
6.5-6.9	0	0	0	0
7.0-7.4	0	0	0	0
7.5-7.9	0	0	0	0
8.0-8.4	0	0	0	0
8.5-8.9	0	0	2	0
Number of Specimens (N)	33	6	155	5
Modal Value	4.7×10^6	3.2×10^6	4.7×10^6	2.7×10^6
Mean Value	3.9×10^6	3.4×10^6	4.3×10^6	3.6×10^6
Standard Deviation	1.0×10^6	1.2×10^6	1.0×10^6	1.0×10^6
Percent Standard Deviation	26%	28%	23%	28%

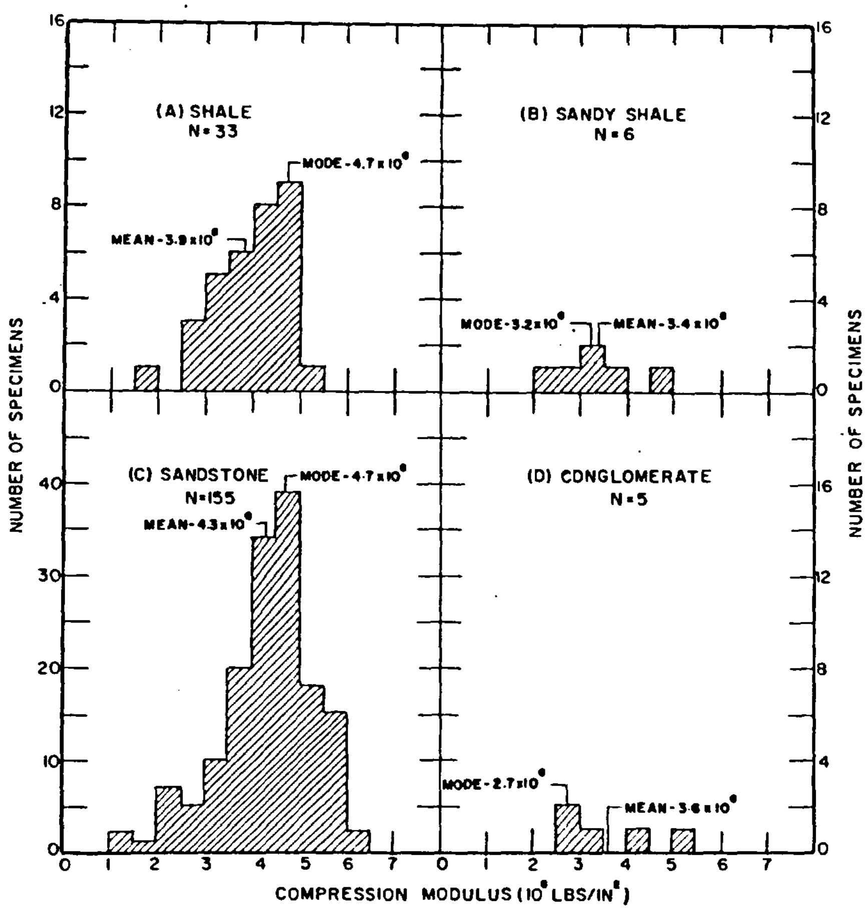

Figure 37 - Distribution diagrams for compression modulus. (McGillivray mine, Coleman, Alberta)

Example: - The following values of ultimate compressive strength were obtained for tests on a set of three shale specimens.

$$X1 = 15.1, \; X2 = 17.2, \; X3 = 13.5$$

Therefore $$\bar{X} = \frac{15.1 + 17.2 + 13.5}{3} = \frac{45.8}{3}$$

$$\bar{X} = 15.3 .$$

<u>Standard Deviation</u> - The standard deviation is a convenient means of expressing the variation in a series of tests. For the simple case, where only a few tests are being considered, the standard deviation may be found from the following formula:

$$\text{Standard Deviation} = s = \sqrt{\frac{(\bar{X} - X1)^2 + (\bar{X} - X2)^2 \ldots + (\bar{X} - Xn)^2}{n-1}}$$

where $\bar{X}$ is the average as found in the previous section,

X1, X2, -- are individual test results, and

n is the total number of test results.

Example: - Using the previous values,

$$X1 = 15.1, \quad \bar{X} = 15.3$$

$$X2 = 17.2, \quad n = 3$$

$$X3 = 13.5$$

$$s = \sqrt{\frac{(15.3 - 15.1)^2 + (15.3 - 17.2)^2 + (15.3 - 13.5)^2}{2}}$$

$$s = 1.8$$

<u>Percent Standard Deviation</u> - The percent standard deviation is defined as follows:-

$$\%s = \frac{s}{\bar{\bar{X}}} \times 100\%$$

Example:- Again using the previous values,

$$\%s = \frac{s}{\bar{\bar{X}}} \times 100\% = \frac{1.8}{15.3} \times 100\%$$

$$\%s \approx 12\%$$

The above values are listed for each physical property at the bottom of the corresponding data sheet (see Table 11).

Significance Tests

By carrying out additional statistical tests on the determined values of the physical properties, it is possible to determine whether apparent differences (for a particular physical property) between two rock types are significant or not. This involves the use of so-called significance tests. Details of these methods are described in text books on statistics, [25] and consequently no details will be given here.

Correlation Diagrams

Where a functional relationship between two variables is suspected, a correlation diagram should be prepared. This involves plotting the two variables, one against the other, for each specimen tested. If, after a sufficient number of specimens have been plotted in this manner, some definite geometric pattern is produced, it would be correct to assume that a definite relationship exists between the two variables. If the mathematical nature of the relationship is required, then standard formulae of statistics (regression) may be

TABLE 12

Data for Correlation Diagram

Compression Modulus Versus Ultimate Compressive Strength (Sandstone, McGillivray Mine, Coleman, Alberta)

Grain Diameter					
0.2 mm down		0.5 mm down		0.8 mm down	
P_u *	E_c **	P_u	E_c	P_u	E_c
25.0	4.9	9.8	2.4	17.0	3.8
26.0	4.8	14.1	2.2	18.0	5.5
26.5	5.5	23.1	5.7	25.4	2.7
27.3	5.3	24.6	4.2	30.8	5.1
27.8	3.8	26.0	6.3	32.0	3.7
28.0	4.2	27.0	4.3	33.0	4.4
28.0	4.6	27.0	2.7	35.8	5.2
28.0	5.1	27.4	5.3	38.0	3.4
32.0	4.0	27.7	4.3	38.8	5.2
37.7	5.5	29.5	4.9		
38.9	4.4	30.4	4.2		
		30.4	2.3		
		32.2	5.1		
		36.8	4.6		
		42.5	5.0		

* P_u - Ultimate compressive strength, $(lb/in^2) \times 10^3$.

** E_c - Compression modulus, $(lb/in^2) \times 10^6$.

applied to gain this information. At present, however, the main interest is whether or not a relationship exists.

There are a number of correlations of particular interest, namely: compression modulus (and ultimate compressive strength, Poisson's ratio, violence of fracture, and fracture angle) versus grain size; compression modulus versus ultimate compressive strength; and violence of fracture versus ultimate compressive strength (and fracture angle). For example, consider the possible correlation between compression modulus and ultimate compressive strength for sandstone specimens from the McGillivray mine. The data are shown in Table 12, subdivided under grain size. Figure 38 shows the resultant correlation diagram. (Little correlation exists in this particular case.)

DISCUSSION

This bulletin has presented the experimental procedures and methods of analysis employed by the Mining Research Section of the Fuels and Mining Practice Division to study the physical properties of mine rock under short-period uniaxial compression.

A considerable amount of such investigation has been carried out. Uniaxial compression data for rocks from six Canadian coal mines and one Canadian iron mine, and for a selected group of rock and mineral specimens from coal and iron ore mines in Europe, are being analysed and will be presented in the manner discussed in this bulletin. The studies of physical properties of mine rock that have been issued to date are:

FRL 243 - Physical Properties of Mine Rock Under Short-Period Uniaxial Compression.

Part (1) - McGillivray Mine (coal), Coleman, Alberta.

Part (2) - International Mine (coal), Coleman, Alberta.

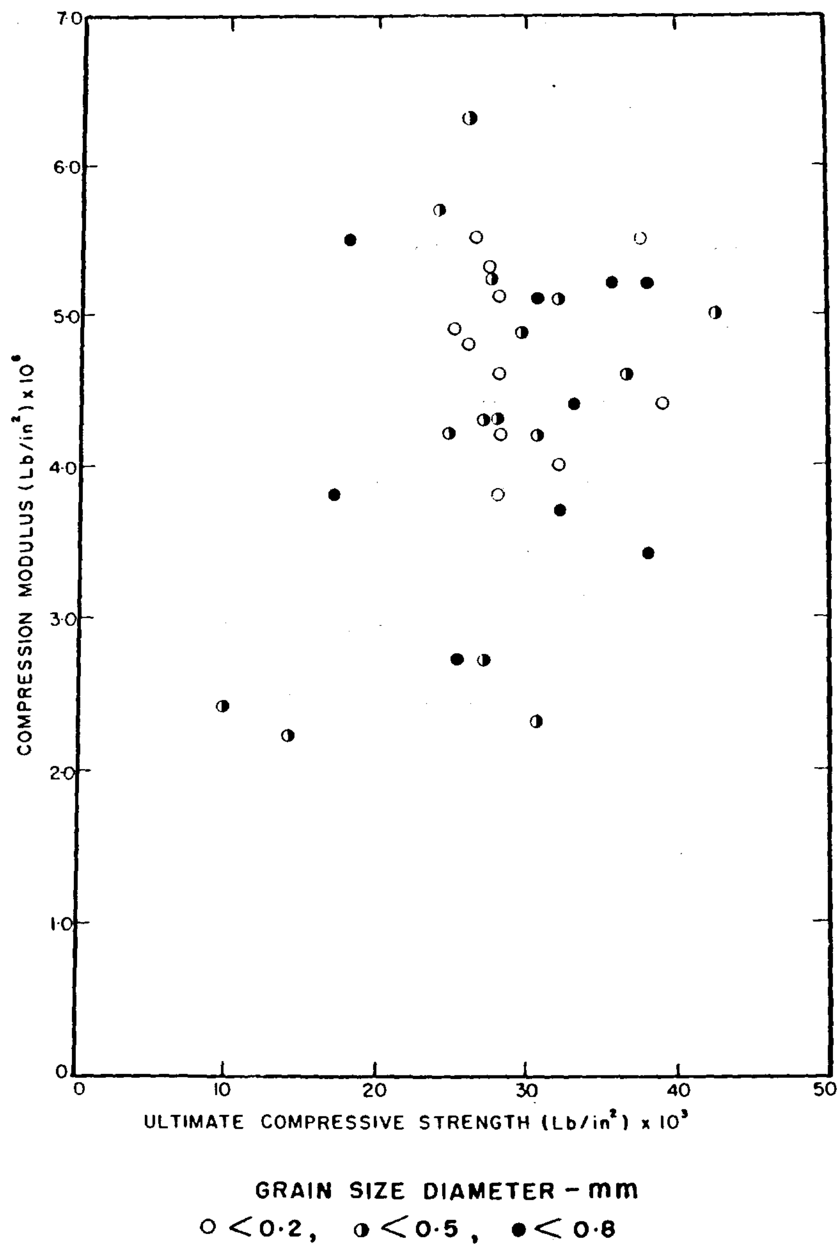

Figure 38 - Correlation diagram of compression modulus versus ultimate compressive strength. (Sandstone, McGillivray mine, Coleman, Alberta)

It is hoped that from a detailed study of these results more light may be shed on the role which the physical properties of mine rock play in the problems of strata control.

ACKNOWLEDGMENTS

Since the investigation of the physical properties of mine rock has been carried out by the Fuels and Mining Practice Division of the Mines Branch over a period of four years and with the constant co-operation of other Divisions, it is felt that the following extensive list of acknowledgments is justified.

The author is indebted to the Physical Metallurgy and Mineral Processing Divisions of the Mines Branch, which made available their testing presses and specimen preparation facilities, and to Dr. K.R. Dawson of the Geological Survey of Canada who carried out petrographic studies on a large number of rock specimens. A great deal of assistance was obtained from other members of the Fuels and Mining Practice Division, particularly M.R. Banville, I.B. David, D.C.K. Ivison, C.R. Laflamme, J.D. Sullivan and A.C. Walker (in specimen preparation, testing, and calculation) and C.A. Vary (in preparing the many graphs and diagrams).

The author is particularly appreciative of the assistance and guidance given by A. Brown, Head of the Mining Research Section, and Dr. W.M. Gray, Division physicist, in carrying out these investigations and in the preparation of this bulletin.

REFERENCES

1. D.W. Phillips, Tectonics of Mining. Colliery Engineering, pages 199-206, 278-282, 312-316, 349-352,and 364-368, 1948.

2. W.I. Duvall, L. Obert, and S.L. Windes, Standardized Tests for Determining the Physical Properties of Mine Rock. R.I. 3891, Bureau of Mines, United States Department of the Interior, 1946.

3. Physical Properties of Some Typical Foundation Rocks, Concrete Laboratory Report No. SP-39, Bureau of Reclamation, United States Department of the Interior, 1953.

4. R.G. Wuerker, The Status of Testing Strength of Rocks. Transactions of A.I.M.E., Mining Engineering, 1108-1113, November 1953.

5. L.U. De Sitter, Laboratory Experiments on Strain of Rock Specimen. Geologie en Mynbouw (English Translation), page 8, January 1952.

6. H. Dukstra, D.W. Van Krevelen, and J. Schuyer, Chemical Structure and Properties of Coal, Part VII, Elastic Constants. Fuel, 33, 407-418, 1954.

7. D.J. Millard, P.C. Newman, and J.W. Phillips, The Apparent Strength of Extensively Cracked Materials. Proceedings of the Physical Society, Section B, page 723, October 1955.

8. F.L. Gaddy, A Study of the Ultimate Strength of Coal as Related to the Absolute Size of the Cubical Specimens Tested. Bulletin No. 112, Virginia Polytechnic Institute, 1956.

9. H.G. Denkhaus and A.J.A. Roux, An Investigation into the Problem of Rock Bursts, Part II. Journal of the Chemical, Metallurgical and Mining Society of South Africa, pages 103-124, November 1954.

10. A. Brown, J.G. Buchanan, E.L. Cameron, H.R. Hardy, Jr., and H. Zorychta, Rock Pressure Studies in the Mines of Springhill, Nova Scotia, A Progress Report. Canadian Mining and Metallurgical Bulletin, 59, 242, 1956.

REFERENCES (Cont'd)

11. H.R. Hardy, Jr., Hardness Tests on Selected Rock Specimens Using the Taber Dyhedron Dynamic Diamond Tester, and their Correlation with other Physical Properties. TM 52/57-MIN, Fuels and Mining Practice Division, Mines Branch, Department of Mines and Technical Surveys, Ottawa, Canada, page 14, 1957.

12. Amsler Mirror Apparatus (Martens System), Type SA 37. Description No. 158, Alfred J. Amsler and Co., Schaffhouse, Switzerland. No date.

13. Baldwin-Lima-Hamilton Corporation Bulletins 225, 279, 279A, 279B, 4450 and 4452. No date.

14. C.C. Perry and H.R. Lissner, The Strain Gage Primer. McGraw-Hill Book Company, Inc., New York, 1955.

15. Van Nostrand's Scientific Encyclopedia. D. Van Nostrand Company, Inc., New York, Second Edition, page 500, 1947.

16. H.R. Hardy, Jr., Studies Conducted to Verify that Stress-Strain Curves for Sedimentary Rocks are Non-Linear. TM 40A/57-MIN, Fuels and Mining Practice Division, Mines Branch, Department of Mines and Technical Surveys, Ottawa, Canada, 1957.

17. W.A. Zisman, Young's Modulus and Poisson's Ratio with Reference to Geophysical Applications. National Academy of Science Proceedings, 19, 660 (1933).

18. H.R. Hardy, Jr., Studies to Correlate the Compression Modulus (and Poisson's Ratio) Values for Mine Rock as Determined by SR-4 Type Resistance Strain Gages and the Marten's Mirror Extensometer. TM 50/56, Fuels and Mining Practice Division, Mines Branch, Department of Mines and Technical Surveys, Ottawa, Canada, 1956.

19. American Society for Testing Materials. Compressive Strength of Natural Building Stone. Tentative Method. A.S.T.M. Designation C170-41T, A.S.T.M. Standards, 1942, Part II, 1102-1104.

20. D.W. Phillips, Tectonics of Mining. Colliery Engineering, page 312, 1948.

REFERENCES (Concluded)

21. S.P. Timoshenko, History of Strength of Materials (McGraw-Hill Book Company Inc., New York, 1953), page 51.

22. F. Birch and P. Le Comte, Dunbar Geophysics Laboratory, Harvard University. Private communication, December 1957.

23. R.O. Bredthauer, Strength Characteristics of Rock Samples under Hydrostatic Pressure. Transactions of A.S.M.E., page 705, May 1957.

24. H.R. Hardy, Jr., Physical Properties of Mine Rock under Short Period Uniaxial Compression, Part 1, Results of McGillivray Mine, Coleman, Alberta. Report No. FRL 243, Fuels and Mining Practice Division, Mines Branch, Department of Mines and Technical Surveys, Ottawa, Canada, 1957.

25. O.L. Davies, Statistical Methods in Research and Production. Oliver and Boyd, Ltd., London, 1954.

....

HRH:(PES):LC

APPENDIX A

Automatic Averaging of Two Strain Gage Readings

The balance condition for the Wheatstone bridge is given in equation (27), namely:

$$R_2 R_d = R_1 R_a \quad \ldots\ldots\ldots\ldots\ldots\ldots\ldots\ldots \quad \text{(i)}$$

and the unbalance due to a change ΔR_a is given by equation (29), namely:

$$\Delta R_2 = (R_1 / R_d) \Delta R_a \quad \ldots\ldots\ldots\ldots\ldots\ldots\ldots \quad \text{(ii)}$$

If the measuring gage R_a is replaced by two separate gages R_a' and R_a'', in series, where $R_a' = R_a'' = R_a$ and R_d is replaced by $2R_d$, then (i) becomes

$$2R_2 R_d = R_1(R_a' + R_a'') \quad \ldots\ldots\ldots\ldots\ldots\ldots \quad \text{(iii)}$$

and therefore

$$R_2 R_d = R_1 R_a .$$

The initial balance condition remains the same. Now in equation (iii), consider a change $\Delta R_a'$ and $\Delta R_a''$ in R_a' and R_a'' respectively,

$$2\Delta R_2 R_d = R_1(\Delta R_a' + \Delta R_a'')$$

$$\Delta R_2 = R_1 (\Delta R_a' + \Delta R_a'')/2R_d \quad \ldots\ldots\ldots\ldots \quad \text{(iv)}$$

Therefore the term $(\Delta R_a' + \Delta R_a'')/2$ replaces the term ΔR_a in equation (ii) and represents the average change in resistance of the two strain gages.

APPENDIX B

Correspondence of Transverse (Diametric) and Circumferential Strains in Cylindrical Specimen

Poisson's ratio has been defined by equation (40) as

$\mu = \Delta e_t \Delta e_l$ where e_t is the transverse strain in the specimen. In a cylindrical specimen the transverse strain would be represented by the diametric strain. In this present series of tests it was not convenient to measure the diametric strain directly. However, the circumferential strain was easily obtained, using attached resistance strain gages.

It is now necessary to determine what relationship exists between the diametric and circumferential strains. Consider a cylinder with diameter d and circumference c.

$$d = c/\pi \quad \text{(i)}$$

An increase Δd in d will result in an increase Δc in c; therefore

$$\Delta d = \Delta c/\pi \quad \text{(ii)}$$

Dividing equation (ii) by (i)

$$\frac{\Delta d}{d} = \frac{\Delta c}{c} \quad \text{(iii)}$$

From equation (iii) it is noted that in a cylindrical specimen the transverse (diametric) and circumferential strains are equal.

= = =

HRH:(PES) LC